



UiT The Arctic University of Norway

Department of Electrical Engineering

Solar Angle Optimizer

Alexander Åkerman

Master's thesis in Electrical Engineering ELE-3900 May 2024



Preface

This master thesis deals with designing, testing and controlling all the components required to make a two axis rotatable solar panel. It uses information and work done in previous related theses to provide detailed information of the requirements for such a system. The purpose of this system is for UiT The Arctic University of Norway campus Narvik to research upon, among other subjects, the efficiency of such a system.

This task was chosen due to my interest in the subject and love for designing and testing electrical components. I would like to extend my sincere gratitude towards the entire staff at UiT Narvik and especially the lecturers for electrical faculty. Over the course of five years they have taught and guided me in my journey in becoming an engineer. I would also like to take this opportunity to extend a special thanks to my supervisor Trond Østrem, senior engineer Ketil Hansen, and senior engineer Johnny Togle for fantastic help during my master's thesis. My supervisor Trond was responsible for assigning me this task, as well as explaining, helping and overseeing the progress and work done during the thesis. Ketil has been a big help in printing circuit boards and buying components required for this thesis. Johnny has been a tremendous help during the practical aspect of this thesis in regards to testing the printed circuit boards produced during this thesis.

Abstract

This thesis deals with the subject of a two axis rotatable solar panel rig where the design for the electrical components are proposed and the controller code from previous theses are further developed. The rig is to be used for research by UiT Narvik and the prerequisites for the installation of the rig are designed in this thesis. The electrical components for the rig proposed are an H-bridge, a power measurement circuit board, and a connection matrix. In addition to the electrical components the code for the controller were changed and a bracket for the induction sensors were designed. The H-bridge was designed, tested and the results obtained were satisfactory. The power supply for the H-bridge which in turn supplies power to the motors were found to be inadequate for its intended purpose with a few possible solutions proposed. The power measurement circuit board was designed, tested and the results obtained during testing were good in regards to accuracy and temperature. The connection matrix was designed but not made or tested. The safety of the design was discussed and a few alternatives were brought up. Positions for the inductions sensors were found and a bracket was designed to hold it. The bracket was not tested but is believed to work as long as the sensors are placed correctly in relation to geographical north. The controller code was further developed but it was not tested extensively in combination with all the other components. Due to the code being developed by multiple people and documentation being vague, the code should be rewritten either partly or fully in addition to further testing.

Contents

1	Introduction	1
1.1	Contributions and scope of the thesis	1
2	Preliminaries	2
2.1	Theoretical preliminaries	2
2.1.1	H-bridge	2
2.1.2	Power measurement	2
2.2	Literature study	3
2.2.1	Mechanical work on the rig	3
2.2.2	Programmable Logic Controller	5
2.2.3	Previous H-bridge design and card	6
2.2.4	Previous power measurement design and card	7
2.2.5	Solar panels	7
2.2.6	Solar tracking method	8
3	Main results	10
3.1	H-bridge	10
3.1.1	Circuit design for H-bridge	10
3.1.2	Simulation of the H-bridge	14
3.1.3	PCB design of H-bridge	15
3.1.4	Testing results of H-bridge	17
3.2	Power measurement card	19
3.2.1	Power measurement Circuit	19
3.2.2	Breadboard test of power measurement circuit	21
3.2.3	Design of power measurement PCB	24
3.2.4	Power measurement PCB test	26
3.3	PLC Programming	27
3.4	Connection matrix	29
3.5	Induction sensor holders	31
4	Discussion	32
4.1	H-bridge	32
4.2	PLC programming	34
4.3	Power measurement circuit board	35
4.4	Connection matrix	35
4.5	Induction sensor holders	36
5	Conclusion	36
5.1	Further work	37
A	Full modified PLC code	40
B	PLC code written in this thesis	50
C	PLC module wiring list	53

D	Relay turn off current graphs	54
E	H-bridge simulation schematic	57
F	Motor start current and voltage	58

1 Introduction

As the demand for renewable energy rises to facilitate the green shift, research into renewable energy systems becomes ever more important. A prominent alternative within the renewable energy sector is solar energy using photovoltaic panels. Solar systems using stationary panels are well documented and used in solar farms already. This thesis is focused on designing and testing a two axis rotating solar system to be used in research into the efficiency of such systems compared to the stationary systems already in use. Rotatable solar systems have the potential to produce more power for longer by positioning the panels perpendicular to the sun for the entire duration of the day based. This type of solar system does, however, consume power to rotate, which leads to research being necessary to determine their efficiency compared to stationary solar systems and other renewable alternatives.

The specific system which is to be designed and tested in this thesis is the result of UiT Narvik's goal of researching solar panels. According to [1] the specific goal of the research is to obtain information on optimal angle of incidence for solar panels during different conditions, which could lead to increased efficiency of solar systems in nordic conditions. Using [1] which details the mechanical construction as well as previous theses done on the topic of solar angle optimization, this thesis will propose and test new designs of electrical components while modifying controller code to interconnect the mechanical and electrical parts of the solar system.

1.1 Contributions and scope of the thesis

The contribution of this thesis is research on solar panels, as explained in the introduction. This thesis' overall goals were to design and test the necessary components to allow the installation of the system. Originally installation and testing of the algorithm were also planned, but due to a lack of time and necessary materials this was altered. The revised goals of the thesis were as follows:

- Redesign the previous H-bridge and test the new design.
- Design and test a power measurement card.
- Propose a design for the solar panel connection matrix.
- Propose a design for the induction sensor holders and position.
- Modify and add functionality to the Programmable Logic Controller (PLC) code.

2 Preliminaries

2.1 Theoretical preliminaries

2.1.1 H-bridge

A H-bridge is a circuit used to facilitate switching polarity to an electrical load. The electrical load for H-bridges are often motors, where the polarity must be switchable to allow for bidirectional movement. A rudimentary H-bridge can be seen in figure 2.1. Upon closing switches S1 and S4 while having switches S2 and S3 opened, the left side of the electrical load will be positive and the right will become negative. Upon closing switches S2 and S3 while having switches S1 and S4 opened, the polarity is reversed, and the right side of the electrical load becomes positive while the left becomes negative. The switches must only be closed in correct pairs while the others are opened, otherwise the input of the H-bridge will be short circuited through the switches.

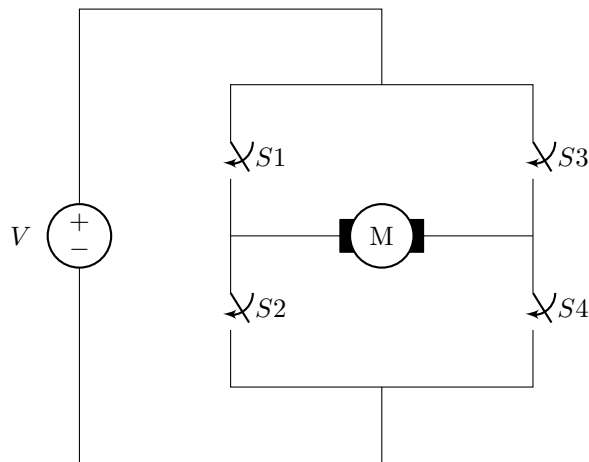


Figure 2.1: Rudimentary H-bridge circuit

2.1.2 Power measurement

Power measurement is the act of measuring the voltage and current in a circuit, and is in this thesis facilitated by using a current transducer and voltage transducer made by LEM. These transducers produce a secondary current proportional to the primary current and by using a resistor on the output will create a voltage proportional to the secondary current. The voltage level is then measured by the analog voltage input module connected to the PLC, which then calculates the voltage and current in the primary circuit. Having knowledge of the power generated by the photovoltaic panels at all times is a critical component used by the PLC to enable the implementation of the perturb-and-observe control algorithm. The transducers both require supply voltages in addition

to the primary and secondary input and output [2, 3]. The circuit used for measuring the power is discussed in section 3.2.3.

2.2 Literature study

2.2.1 Mechanical work on the rig

The mechanical considerations and design of the system were done in [1], and this entire paragraph uses information from their thesis. In the thesis a design for the frame, an adapter plate, as well as how to enable two axis movement of the rig were discussed. The frame's function is to hold all the solar panels and mount to the two axis slewing motor drive. The thesis did a structural analysis of the proposed design for the frame where it was concluded that it would satisfy the strength requirements considering wind and snow load. The frame has not yet been manufactured, meaning only simulation data exists at present time. Figure 2.2 taken from [1] displays a model of the frame. In addition to the frame an adapter plate was made so that the two axis slewing motor drive could be mounted on top of a concrete mast. Figure 2.3 also taken from [1] displays the model for the adapter plate with the left side showing the top of the adapter plate, and the right side showing the bottom of the adapter plate. The final mechanical question discussed is how to implement dual axis movement for the rig. Several solutions to this were discussed in regards to the solar tracking application, where the thesis found that a commercially available two axis slewing drive made by Kinematics was the best choice. According to [1] it was chosen due to easily satisfying the requirements, as well as being the cheapest solution discussed. The specific model bought for the rig is SDE7D-73MHA-24H01RC-BA160, which can be seen in figure 2.4. This model uses two 24V DC motors connected to worm gears to enable movement in two axes with a speed of 0.12 rpm. It also has Hall-sensors which gives feedback of motor positioning with a resolution of 191.42 points per degree of movement in both azimuth and tilt direction. A model of the complete mechanical system can be seen in figure 2.2.1, which is also obtained from [1].



Figure 2.2: Frame designed in [1]

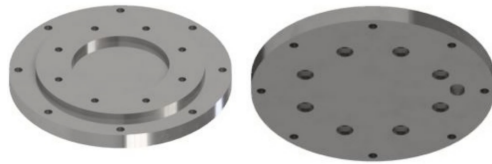


Figure 2.3: Adapter plate designed in [1]

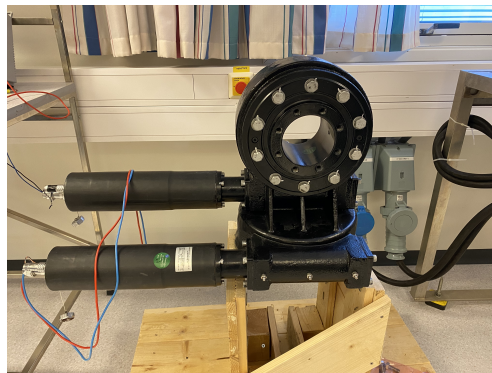


Figure 2.4: Two axis slewing motor drive bought for the rig.

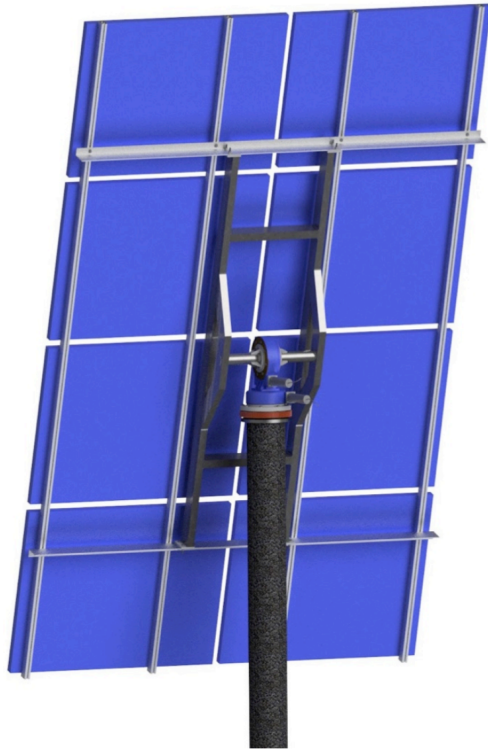


Figure 2.5: Model of complete mechanical setup taken from [1].

2.2.2 Programmable Logic Controller

A programmable logic controller is a modular programmable controller that can perform actions based on its programming and available modules. The PLC used to implement solar tracking in this thesis was the WAGO PFC200 with several analog input and output modules to facilitate physical control of the solar panel rig. The following modules have been connected with the main controller: two frequency counters, two analog input current modules, a digital output module, a real time clock module, four analog input voltage modules and an end module. Some of these modules are excessive as only seven of the eleven modules are actually required to implement the control system. The following modules are required: two frequency counters, one analog input current module, two analog input voltage modules, a digital output module, and an end module. Figure 2.6 obtained from [4] which is a thesis on the same subject shows the required WAGO modules and their connections. Similarly, [4] also provided a detailed wiring list which can be seen in appendix C. Following the wiring list is essential to ensure correct interface between the PLC programming and the hardware if the unmodified code from [4] is to be used.

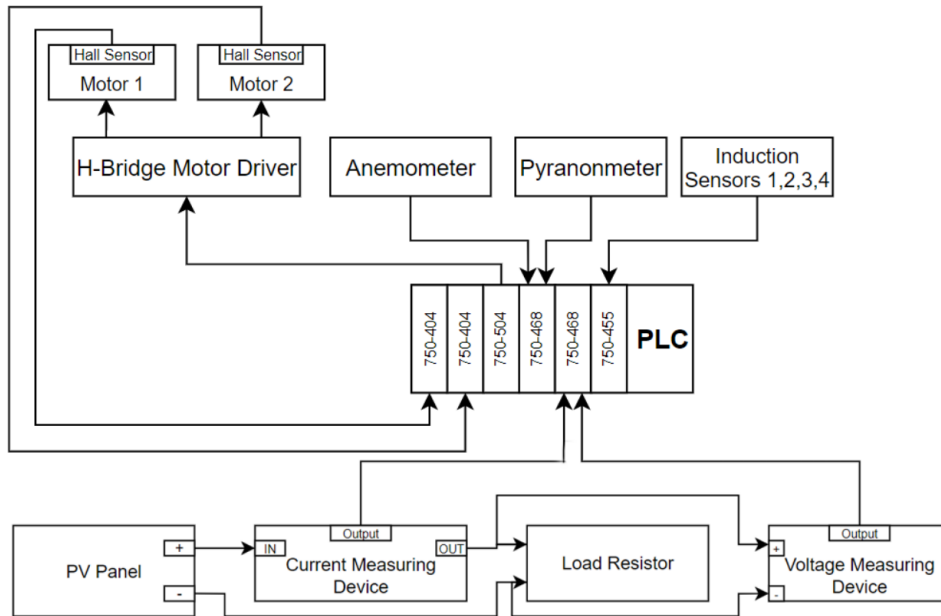


Figure 2.6: PLC modules and their connections obtained from [4]

2.2.3 Previous H-bridge design and card

There have been at least two different H-bridges designed in previous theses covering the same topic as this thesis. The two known H-bridges were designed in [5] and [4]. In [5] a design with capacitors over the relays was made with a recommendation of adding free-wheeling diodes over the inductor coils of the relays. The design utilized four HF140FF-024-2HTF double pole single throw normally open relays, four unspecified two pin Printec Circuit Board (PCB) terminal blocks and four unspecified non-polarized capacitors for one H-bridge [5]. A PCB using this design was made, but due to faults with the relays no testing was conducted [5]. In [4] the H-bridge was redesigned with fewer components. The new design used the same relays as the previous one, and comprised of two relays and four two-pin PCB terminal blocks for one H-bridge [4]. The design uses two identical H-bridges, one for each motor, where each one is connected similarly to figure 2.1 using one relay in place of two switches [4]. In the conclusion and further work section of [4] it was stated that the H-bridge had to be redesigned once more. A PCB using this design was created, but no testing data was documented for it. Due to the first design being faulty and unavailable, and the second design lacking capacitors and free-wheeling diodes, it was decided that the H-bridge would be redesigned in this thesis.

2.2.4 Previous power measurement design and card

In [5] a power measurement circuit and PCB design are proposed, and in [4] this design is tested. The design uses two LEM elements of type LAH 50-P and HX 03-P with unspecified resistors to allow for correct scaling to the PLC [5]. In Skjelbred's thesis the circuit is not tested in regards to known input voltages and currents, but in [4] this is done. The thesis seen in [4] documents the circuit measurement values on input voltages of 10V to 42V and on currents of 1.2A and 2.63A using resistors with values of 390Ω , $22k\Omega$, and 150Ω . Following the test, [4] stated that the current measurements were accurate, while the voltage measurements were inaccurate for low voltages [4]. It is stated in both theses that the circuit is not able to be used with all eight solar panels [5, 4]. Due to the design being unable to measure the power from all eight panels, it was decided that the circuit and PCB were to be redesigned in this thesis.

2.2.5 Solar panels

The rig will initially utilize eight identical solar panels, with the specifications for each of these shown in table 2.1. Maximum power generation for each panel is 200W, with maximum power voltage being 36.5V and maximum power current being 5.48A. Depending on the connection of all eight panels the voltage can be a maximum of 292V and the current can have a maximum of 43.84A while connected to an electrical load. When the panels are not connected to a load the voltage can be a maximum of 356V which could be relevant in regards to safety and voltage ratings of connected components. During a short circuit the current of the panels can be a maximum of 47.36A which could be relevant in regards to the current ratings of components used. To allow for different panels in the future, and to have some margin, the power measurement card connected to the solar panels will be designed with a voltage rating of 400V and a current rating of 50A.

Table 2.1: Solar panel specifications

Model Name	SNM-M200(72)
Maximum Power (Pm)	200W _p
Open-Circuit Voltage (Voc)	44.5V
Short-Circuit Current (Isc)	5.92A
Maximum Power Voltage (Vmp)	36.5V
Maximum Power Current (Imp)	5.48A
Maximum System Voltage (V)	1000VDC
Temperature System Voltage	-40 ° C to +85 ° C
Tolerance	+/-3%
Weight	15.5Kgs

2.2.6 Solar tracking method

Solar tracking is a core concept in this thesis which refers to the solar panel rig's ability to position itself perpendicular to the sun at all times to maximize power generated by the solar panels. The perturb and observe algorithm used in this thesis is implemented by using a power measuring PCB, induction sensors and a PLC. The power measuring PCB supplies data to the PLC for use in the optimization algorithm. The induction sensors are used to limit excessive movement which would result in damage to the system, and to determine initial position of the solar panels. The PLC is used as a central controller which utilizes all the data from all the other components to calculate necessary data and determine the rig's next course of action. The PLC's response is decided based upon sensor data and the perturb-and-observe algorithm. The algorithm is a simplistic algorithm which compares the power generated in two different operating points to determine movement. Obtaining the power generated in one operating point, the operating point is slightly changed by moving the solar panel position, where power from the new operating point is measured. If the second operating point yields a larger power generation than the first, the rig will continue in that direction until it no longer increases. However, if the second operation point decreases instead, the rig will move in the opposite direction until power generation stops increasing. After the optimal power point has been found the rig will stay idle for a set amount of time before optimizing once more. The entire process continues in an endless loop and is done on each motor separately, meaning that the optimization process is first conducted on motor 1 before the same process is done with motor 2 [4]. The PLC code which implements this algorithm also contains other states to reduce the likelihood of damage. In figure 2.7 obtained from [4], an overview flowchart of the PLC's programming can be seen [4]. The flowchart gives a good overview of the states

and actions of the solar rig during operation.

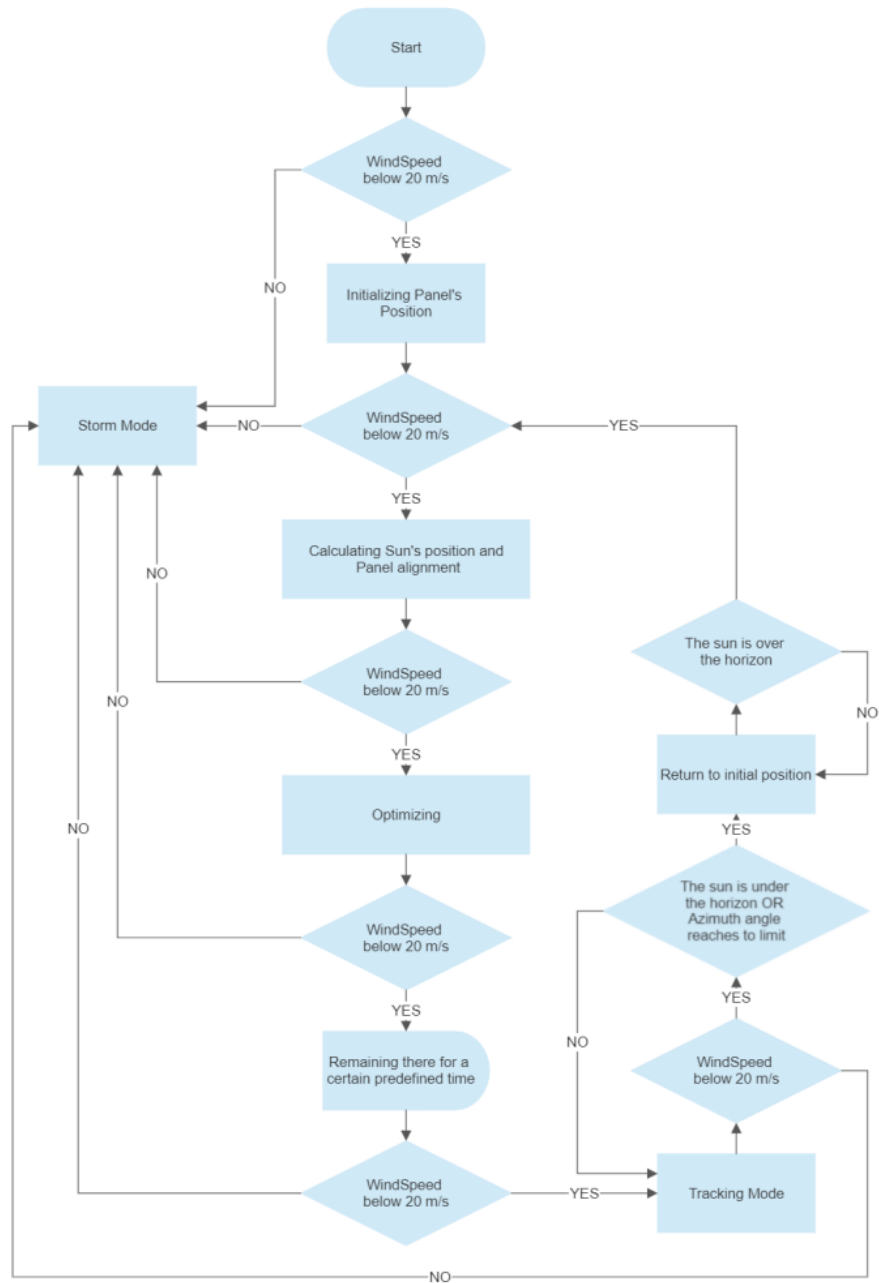


Figure 2.7: PLC code overview flowchart [4]

3 Main results

3.1 H-bridge

3.1.1 Circuit design for H-bridge

The H-bridge was redesigned to include capacitors, free-wheeling diodes and fuses to increase reliability and safety compared to previous designs. The design uses four relays, eight capacitors, four diodes and seven two-pin PCB terminal blocks. The simplified circuit is shown in figure 3.1 where the relays have been substituted for individual switches instead, which as a result omits the free-wheeling diodes as well. Four relays of model HF140FF/024-2HTF are used in the design, which according to an appendix in [4] states that they are double pole single throw 24V relays with a max switching current of 10A [4]. Eight capacitors are used in parallel over the switches of the relays to reduce the voltage spike that occurs when abruptly disconnecting an inductive load. All eight capacitors used in the H-bridge are polarized 68 μ F with a $\pm 20\%$ tolerance and a voltage rating of 25V DC [6]. One diode of type 1N4007 is placed in anti-parallel with the induction coil on each relay to reduce the voltage spike that otherwise would occur in the PLC control circuit. The PCB terminal blocks used are RS PRO 2-contact terminal block with a current rating of 16A [7]. The fuse holders used are Schurter 5x20 mm holders with a current rating of 10A and a voltage rating of 250V AC [8]. Schurter slow-blow ceramic 5x20 mm 10A fuses are used in the holder. The power supplied used to operate the motors is an OMRON S8VK-C48024, with an output voltage of 24V and maximum output current of 20A [9]. The full circuit for the new H-bridge design is shown in figure 3.2.

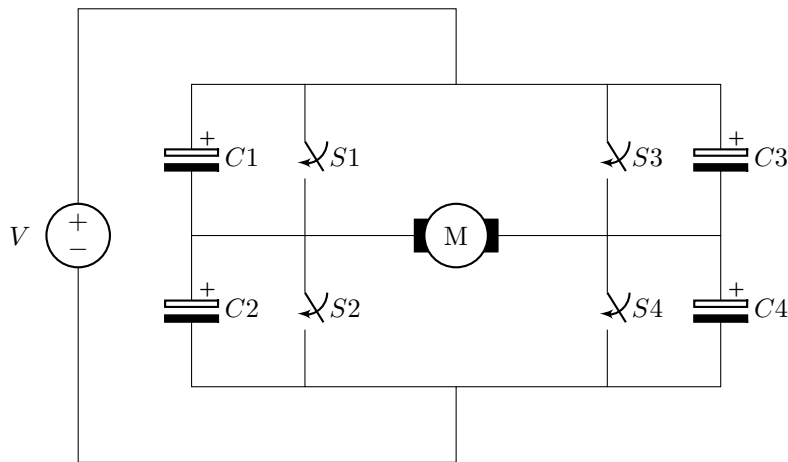


Figure 3.1: H-bridge circuit

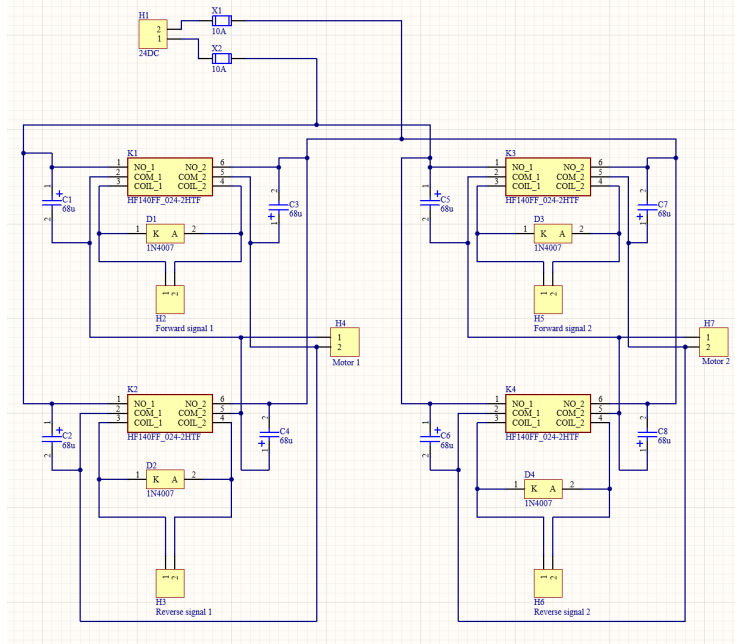


Figure 3.2: H-bridge schematic as seen in Altium Designer

The capacitance value required to mitigate the voltage spike upon switching off a relay was calculated in three ways where the first method involves using equation 3.1 and equation 3.2.

$$Q = i * t \quad (3.1)$$

$$C = \frac{Q}{V} \quad (3.2)$$

Appendix D shows the motor current during three separate tests where the relay in the H-bridge is switched off. The current used in equation 3.1 was chosen as the highest recorded current in each experiment to obtain a minimum capacitance value and the time was chosen based on the aforementioned figure. The results is then used in equation 3.2 with V being 12. The average capacitance obtained from the three tests are multiplied by two to obtain a minimum capacitance value under worst case scenarios, which in turn serves as the capacitance value calculated using these equations. The value calculated for required capacitance of the capacitors using these equations is $3.21 * 10^{-5}$ F.

The second way of calculating required capacitance involves using figure 3.3 to approximate the derivative of the current upon starting the motor. Using equation 3.3 to calculate motor inductance then using the absolute value in equation 3.4 with I as 2 A due to it being the typical no-load current, and then

using this result in equation 3.5 the minimum capacitance can be approximated to $1.09 * 10^{-5}$ F.

$$\epsilon = -L * \frac{dI}{dt} \quad (3.3)$$

$$W = \frac{1}{2} * L * I^2 \quad (3.4)$$

$$W = \frac{1}{2} * C * V^2 \quad (3.5)$$

The required capacitance with margins for error is the double of this at a capacitance of $2.18 * 10^{-5}$ F. A current of 2 amperes was used in the calculation as this is the no-load typical current drawn from the motors during normal operation. This number might have to be adjusted to accommodate the increase in current drawn due to increased load on the motors, but due to the rig being incomplete the actual current drawn is uncertain due to motor characteristics, variable mechanical load and gearing. To find a suitable value to use as I in the equations, the current drawn when the rig is in full operation must be found before the equations are used to calculate the new capacitance required.

The third way to obtain the required capacitance value involves measuring the motor's inductance and using equation 3.4 and equation 3.5. LCR measurements of the motors at 1kHz give inductance values of 888.1 μ H and 857.1 μ H, respectively. The LCR measurement is shown in figure 3.4. Using the largest measured value of the motors then inserting it into equation 3.4 while using current as 2A the energy can be calculated. Using the calculated energy in equation 3.5 with voltage as 24V the minimum capacitance is calculated to a value of $6.17 * 10^{-6}$ F. The required capacitance with margins for error is double this at $1.23 * 10^{-5}$ F. This method can be done purely theoretical if given the motor inductance from manufacturer, but due to a lack of this data the inductance was measured instead. The minimum required capacitance for the motors in this configuration is selected to be the highest of the three methods to ensure the continued mitigation of the voltage spike under all conditions. Using capacitors with a capacitance of 68 μ F exceeds the minimum requirements by a factor exceeding two as a higher capacitance carries no inherent negative consequences for performance.

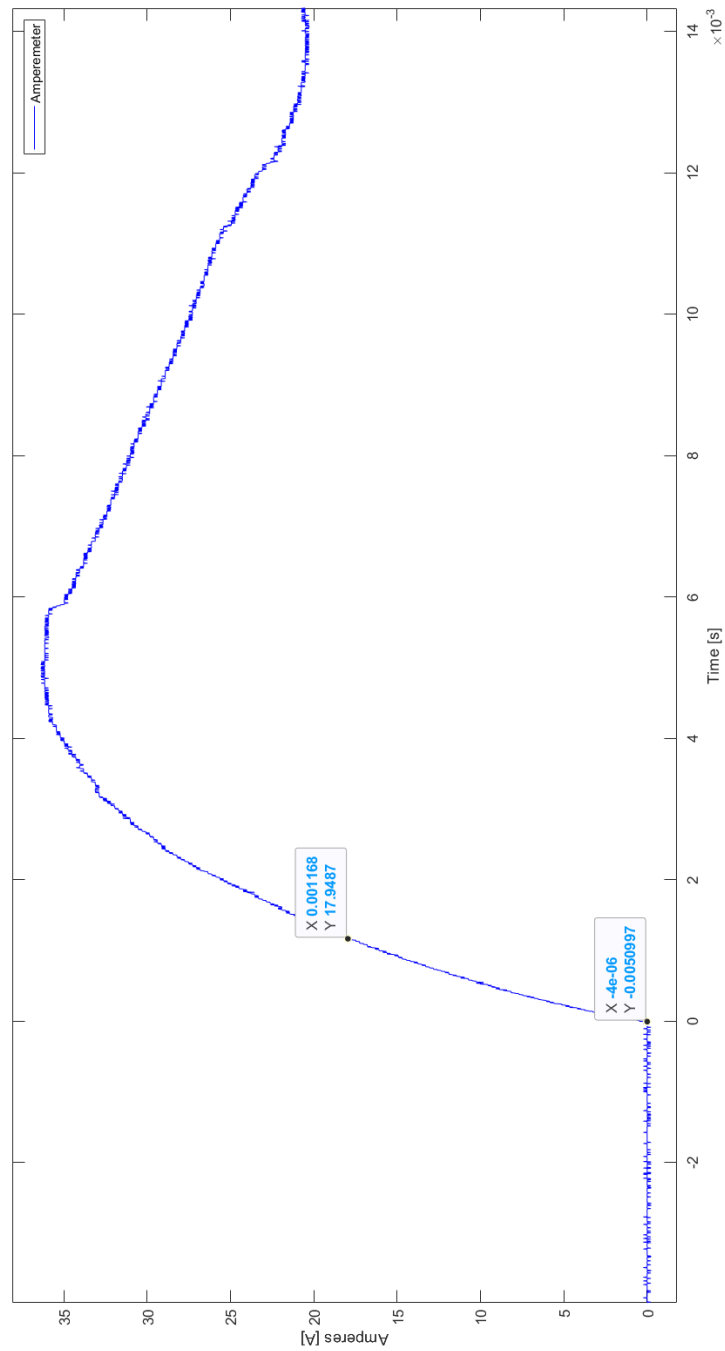


Figure 3.3: Motor start up current

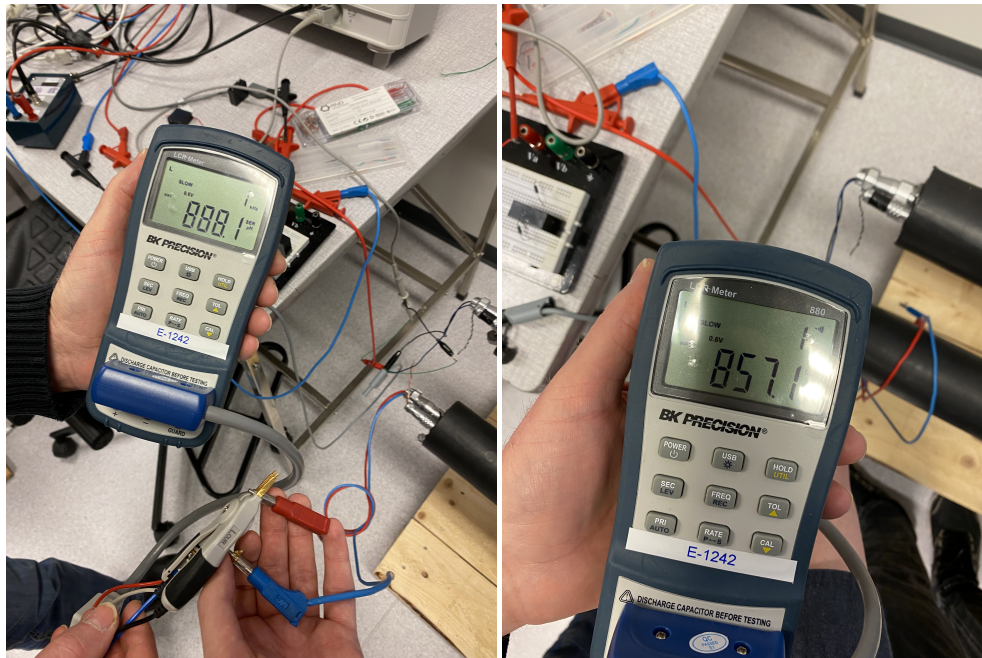


Figure 3.4: LCR meter inductance testing of motors

3.1.2 Simulation of the H-bridge

The H-bridge was simulated using Altium Designer where the relays were replaced with a double-pole single throw generic relay with default values. The schematic made for the simulation is shown in appendix E, while the simulation results are shown in figure 3.5. The simulation results shows that the circuit works as intended and that the voltage over the relay switch will only spike to 24.5V. The simulation is not very accurate as the parameters set for the relays and motors are not the same as the actual components but they verify the functionality of the H-bridge.

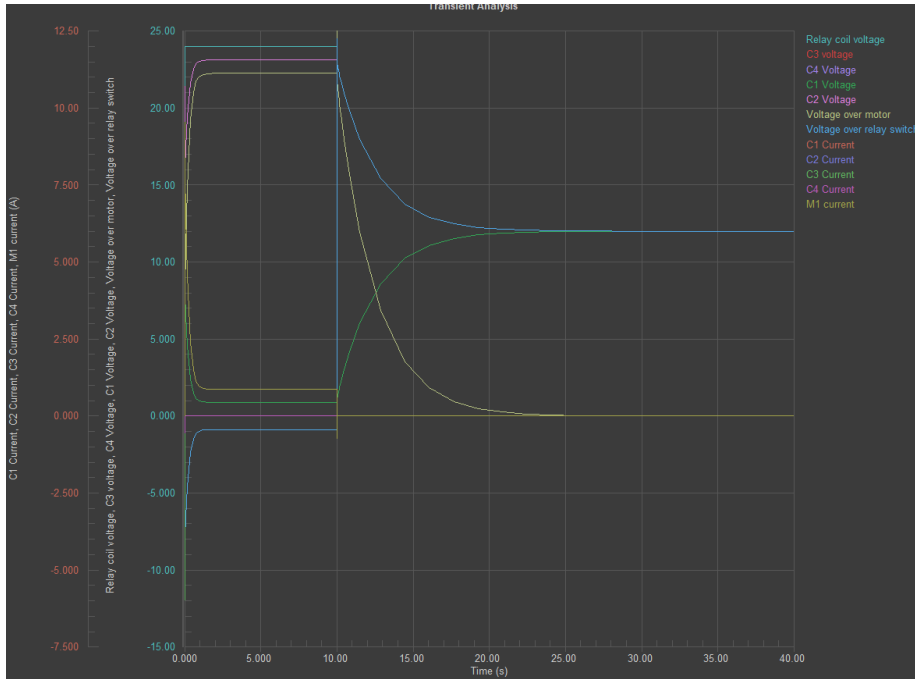


Figure 3.5: H-bridge simulation results from Altium Designer

3.1.3 PCB design of H-bridge

The PCB was designed with a current rating of 10A and had a focus on minimizing temperature with a spacious design. The main track width used to transfer power to the motors is dimensioned for 11 amperes due to the motor datasheet seen as an appendix in [4] stating current draw to be $\leq 11A$. Although the main tracks are dimensioned for 11A, the relays and fuse holders are limited to 10A thus reducing the overall current rating to 10A. The track width of the main power routes was 209 mils, the track width to the capacitors are 92 mils based on simulation data and the track width to the relay coils are 50 mils. An online calculator published on Altium Designer’s website, as well as an internal calculator inside Altium Designer, were used to choose an adequate track width size. On both calculators the following parameters were selected or used as standard: 20 degrees temperature rise above ambient on an external track with a copper weight of 1 oz/ft², which is a copper thickness of 0.013inches, or 33 μ m [10]. According to the online calculator and the calculator within Altium Designer a 209mils wide track can have 11.009A going through it, a 92 mils track can have 6.073A going through it and a 50 mils track can have 3.903A going through it [11]. The online calculator published on Altium Designer’s website and the internal calculator in Altium Designer itself are both based upon the IPC-2221A standard [11]. Due to a lack of access to the IPC-2221A standard this could not be verified directly from the source. A newer standard also detailing information

on PCB track width, current and temperature is the IPC-2152 standard. The standard provides charts in both imperial and metric units, where metric is the expected choice, however, due to being taught in imperial units this is used [10]. According to figure 5-2 in the IPC-2152 standard a 10A current draw requires a cross-sectional area of 500 mils to rise 20 degrees Celsius above ambient [10]. Also according to figure 5-2 the track width required when using a 1-oz PCB is ≈ 0.38 inches wide or 380 mils to obtain a cross-sectional area of 500 mils [10]. Repeating the same steps using figure 5-6 a similar width size can be found [10]. According to IPC-2152 itself the track width is usually an overestimation of what is actually needed to achieve the temperature stated [10]. The vias used to make an electrical connection between the top and bottom layer were made using $2.5mm^2$ conductor taken from a PR cable. Following table 52A-2 in NEK 400:2022 the closest installation method to the environment on the PCB was number 42 meaning reference installation method B2 can be used to find current carrying ability [12]. Following table 52B-2 in NEK 400:2022 the current carrying ability for a $2,5mm^2$ two-core PVC-isolated copper wire using installation method B2 is 23 amperes with a 70 degree Celsius wire temperature and 30 degree Celsius ambient temperature [12]. The wire used as vias on the PCB are far shorter, is covered in tin, has only one wire and no PVC isolation when compared to the cable described in the table, which leads to an unknown increase in current carrying ability, which in turn guarantees the performance when 10A is going through it. According to table 6-1 in IPC-2221B the minimum spacing between tracks on a bare printed board using method B2 with a voltage of 16-30V between conductors is 0.1mm [13]. All models and footprints used in this PCB layout were self-made with the exception of the relays, which were obtained from Rapidoonline [14].

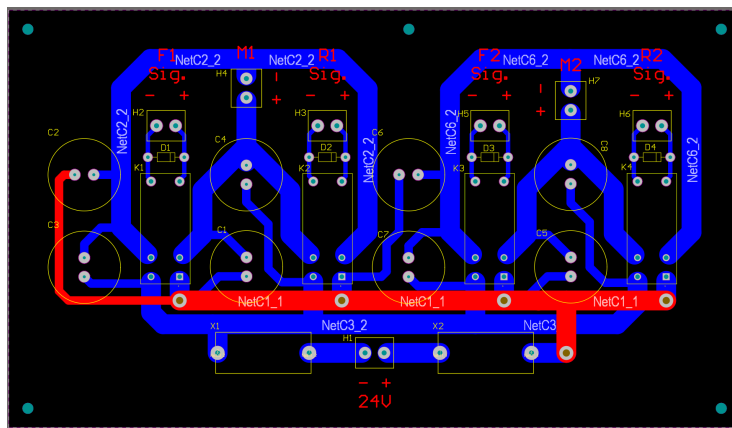


Figure 3.6: H-bridge PCB layout as seen in Altium Designer

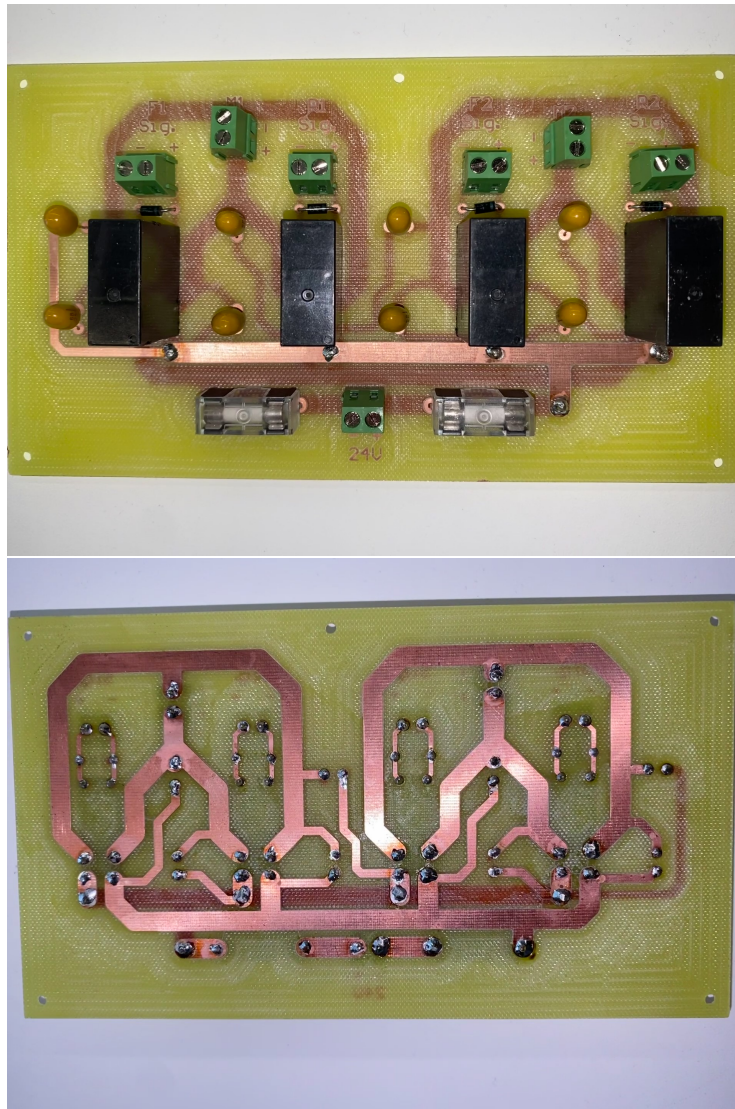


Figure 3.7: H-bridge complete PCB

3.1.4 Testing results of H-bridge

The H-bridge circuit was first tested on a trainer board before being tested as a finished PCB to verify the performance. The trainer board test was to verify the functionality of the circuit, and the results from this are similar to the final PCB. The PCB was tested after the trainer board test and the PCB design process to verify that there was no voltage spike upon opening the relay. The voltage across a relay switch when the relay closes is shown in figure 3.8 while

the voltage across the same switch when the relay opens is shown in figure 3.9. The oscilloscope data shows that no voltage spike occurs when opening the relay, which will serve to lengthen the lifespan for the relays. Due to switching noise in the setup when testing the free-wheeling diodes the measurement data was invalidated and it is unknown how big of an impact they have in protecting the PLC module. The conclusion in regards to the H-bridge is that the capacitors functions as intended, and the PCB is able reversed the polarity of both H-bridges and run a motor without any issues.

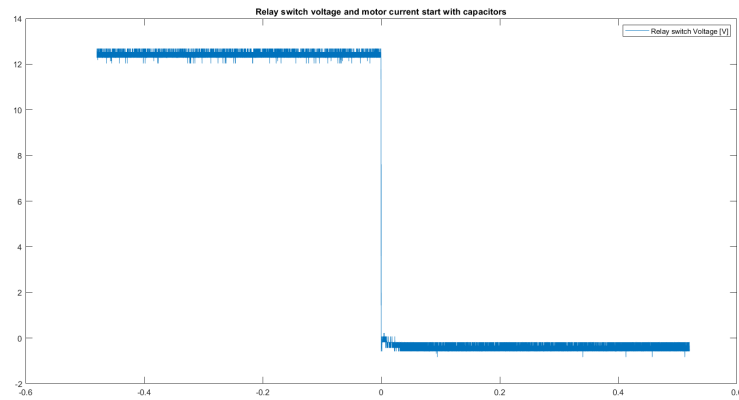


Figure 3.8: H-bridge PCB relay switch voltage when starting the motor

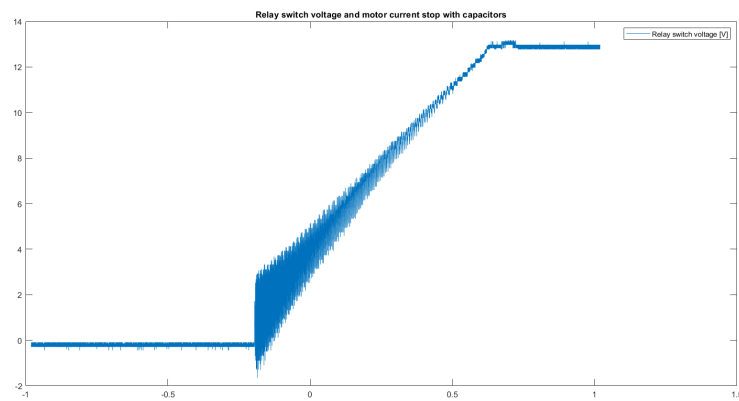


Figure 3.9: H-bridge PCB relay switch voltage when stopping the motor

3.2 Power measurement card

3.2.1 Power measurement Circuit

The power measurement circuit was designed with a voltage rating of 400V and a current rating of 50A. The components used are LEM elements LV 25-P and LA 55-P, a RAC20-15DK power supply, one 150 Ω resistor, one 330 Ω resistor, four 10k Ω resistors, three fuses with holders and four PCB terminal blocks. The complete circuit used for measuring power is shown in figure 3.10 while the schematic made in Altium Designer is shown in figure 3.11. The LV 25-P voltage transducer is suitable for measuring voltage levels between 10V and 500V with a primary nominal current of 10mA and a supply voltage between $\pm 12V$ and $\pm 15V$. [3]. LV 25-P was chosen due to easy access, having a measuring area suitable for this purpose, good accuracy and linearity, and having a low current consumption. The LA 55-P current transducer is suitable for measuring currents up to 50A using a supply voltage between $\pm 12V$ and $\pm 15V$ [2]. LA 55-P was chosen over other current transducers due to easy access, and to avoid having 50A going through the PCB due to space and temperature concerns, and instead have a wire go through it. The RAC20-15DK power supply uses an input of 230V AC and gives an output of $\pm 15V$ DC which is used as the power supply for the LEM elements [15]. The 150 Ω resistor which is placed in the secondary circuit of the LA 55-P component has part number ER74150RJT and was chosen due to high precision, high power rating and low thermal drift. The resistor is a 3W 150 Ω with a tolerance of $\pm 5\%$, a voltage rating of 100V and a typical temperature coefficient of 0-60ppm/ $^{\circ}C$ [16]. The 330 Ω resistor which is placed in the secondary circuit of the LV 25-P has part number LR1F330R and was chosen primarily due to high precision and low thermal drift. The resistor is a 0.6W 330 Ω with a tolerance of $\pm 1\%$, a voltage rating of 350V and a temperature coefficient of 50ppm/ $^{\circ}C$ [17]. The voltage rating of the resistors placed in the secondary circuit of the LEM elements is not of importance, as the secondary circuit will have a maximum voltage of 10V due to the PLC analog voltage input module limitations. The four 10k Ω resistors which are placed in the primary circuit of the LV 25-P has the part number 45F10KE, and were primarily chosen due to high precision, high power rating and low thermal drift. The resistors are 5W 330 Ω with a tolerance of $\pm 1\%$, a voltage rating of 460V and a temperature coefficient of ± 20 ppm/ $^{\circ}C$ [18]. Due to high power dissipation in the resistors placed in the LV 25-P component's primary circuits, four 5W 10k Ω resistors were placed in series instead of a singular 5W/10W 40k Ω resistor to reduce the temperature of the resistors. All resistors used in the design have a low temperature coefficient as the ambient temperature around the card is unknown and varies, leading to an unknown error in the power measurements. A low temperature coefficient for the resistors will aid in keeping the measurement error lower for varying ambient temperatures and power generation from the solar panels and thus power dissipation in the resistors. The fuse holders has part number 0031.8211, a voltage rating of 250VAC, a current rating of 10A and holds 5x20mm fuses [8]. The fuses are slow blow fuses from Schurter, and

their values and types are shown in figure 3.11. The PCB terminal blocks used as connectors for the cards has part number 1890963, and a voltage rating of 400V, a current rating of 16A with a nominal wire cross section of $2,5mm^2$ [19]. The resistors placed in series with both LEM elements' primary circuit and the resistor placed in series with the secondary circuit are calculated to obtain a primary and secondary current suited for the PLC and the required voltage rating. Using ohm's law combined with the turns ratio between the primary and secondary circuit in the LEM elements the required resistor values can be calculated. Using 400V as nominal voltage from the solar panels in the calculations for the LV 25-P component $40k\Omega$ resistors in the primary circuit yields a primary current of 10mA. Following the turns ratio of 2500/1000 the secondary current will be 25mA, and the secondary voltage will be 8.25V when using a 330Ω resistor. Using the equation for power calculation, the power dissipation for the primary side is 4W and 0.20625W for the secondary side. The datasheet for the primary side resistors lack a load vs temperature chart to determine temperature, but the datasheet for the resistors on the secondary side show a temperature increase of about $20^\circ C$ with a load of 0.20625W [18, 17]. The calculations for the LA 55-P component is similar, and using a primary nominal current of 50A the secondary current becomes 50mA due to the turns ratio of 1/1000. The voltage on the secondary side then becomes 7.5V with a power dissipation of 0.375W, which the datasheet says a temperature increase of about $20^\circ C$ is expected [16]. The PLC analog input module can read values of $\pm 10V$ which can mean higher resistance values can increase resolution of the measurement. This was not done as the datasheets for LV 25-P and LA 55-P state a maximum measuring resistor value of respectively 350Ω and 160Ω when using a supply voltage of $\pm 15V$ and the limitations set [3, 2]. The circuit was tested on a breadboard before printing a circuit board, but a simulation could not be done as the LEM elements' behavior lacked a spice simulation model.

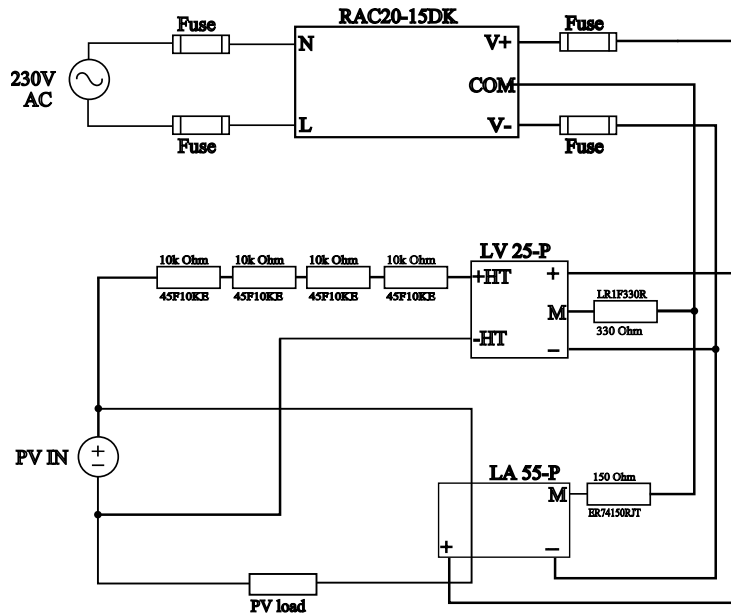


Figure 3.10: Power measurement circuit

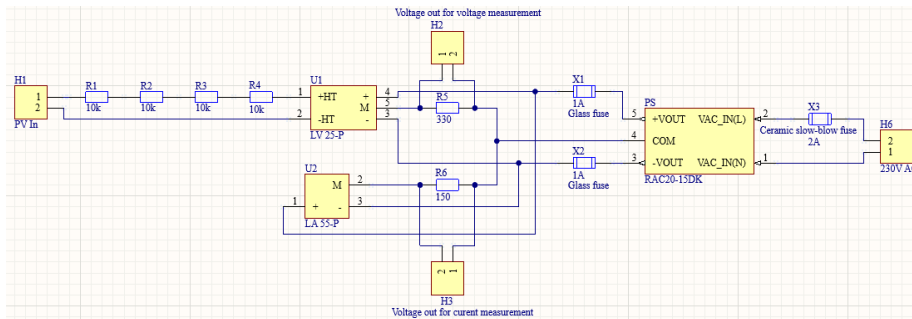


Figure 3.11: Power measurement schematic

3.2.2 Breadboard test of power measurement circuit

Due to a lack of simulation data the power measurement circuit was tested on a breadboard with generic components to verify the functionality of the design before a PCB was made. Due to limitations in testing equipment the test was only conducted with a maximum voltage of $\approx 250\text{V}$ and a maximum current of $\approx 50\text{A}$. The measuring resistor used in voltage measurement had a resistance value of 378Ω which was measured using a multimeter. The load resistor had a given value of $39\text{k}\Omega$, but was not checked with a multimeter. Measuring the exact value of both resistors and using that in the equations instead of the given

value will yield an increase in accuracy of the measurement, but is not necessary nor important for the tracking algorithm as it does not depend upon specific values. Table 3.1 shows the test results obtained for voltage measurement via the PLC. The data out of the PLC changed slightly every data log sample and an estimate was made for the results. The raw data from the PLC is converted to voltage using equation 3.6, where the fraction value is obtained from the module manual [20] seen in table 3.2.

$$V_{PLC} = \frac{d}{32760} * 10 \quad (3.6)$$

Where V_{PLC} is the input voltage to the PLC module and d is the raw data given from the module to the PLC code.

The converted PLC input voltage is converted into the simulated solar panel input voltage by using equation 3.7.

$$V_m = \frac{V_{PLC}}{R_m} * \frac{1000}{2500} * R_L \quad (3.7)$$

Where V_m is the measured input voltage, R_m is the measuring resistor in the secondary circuit of the LEM elements, and R_L is the total resistance in the primary circuit of the LEM elements.

Measurement error to check accuracy is calculated by using equation 3.8.

$$Error = \frac{V_m - V_{Supply}}{V_{Supply}} * 100 \quad (3.8)$$

Where the Error is the measurement error in percentage, and V_{Supply} is the actual supplied voltage.

Table 3.1: Voltage measurement results

Supply voltage to be measured [V]	PLC input voltage (multi-meter measurements) [V]	PLC input voltage (PLC measurements) [V]	PLC voltage measurements of supply voltage [V]	Measurement error in percentage [%]
10.1	0.259	0.26	10.7	5.94
30.0	0.730	0.73	30.3	1
60.04	1.442	1.44	59.6	-0.73
100.11	2.392	2.39	98.8	-1.31
199.24	4.733	4.73	195.2	-2.03
248.85	5.904	5.89	243.4	-2.19

Table 3.2: WAGO module manual showing raw data values out corresponding to input voltage [20]

Input voltage 0V .. 10 V	Numerical value				Status-byte hex.
	Binary value	*)XFÜ	Hex.	Dec.	
<0.00	'0000.0000.0000.0	000'	0x0000	0	0x00
0.00	'0000.0000.0000.0	000'	0x0000	0	0x00
1.25	'0001.0000.0000.0	000'	0x1000	4096	0x00
2.50	'0010.0000.0000.0	000'	0x2000	8192	0x00
3.75	'0011.0000.0000.0	000'	0x3000	12288	0x00
5.00	'0100.0000.0000.0	000'	0x4000	16384	0x00
6.25	'0101.0000.0000.0	000'	0x5000	20480	0x00
7.50	'0110.0000.0000.0	000'	0x6000	24576	0x00
8.75	'0111.0000.0000.0	000'	0x7000	28672	0x00
10.00	'0111.1111.1111.1	000'	0x7FF8	32760	0x00
>10.00	'0111.1111.1111.1	001'	0x7FF9	32761	0x42

*) status bits: X = not used, F = short-circuit, Ü = oversize

Table 3.3 show the results of current measurement using the PLC. Measurements are taken using a resistor with a measured value of 187Ω . The raw data from the PLC is converted to voltage using equation 3.6. The supply current was calculated using equation 3.9.

$$I_m = \frac{V_{PLC}}{R_m} * \frac{1000}{1} \quad (3.9)$$

Where I_m is the measured current, V_{PLC} is the input voltage to the PLC module, and R_m is the measuring resistor in the secondary circuit of the LEM element.

To limit current draw during the experiment and to ensure that the LEM element could measure the current specified in the design section, the wire is wound five times through the LEM element. This results in the LEM element measuring five times the actual current and subsequently means the results obtained from the experiment has to be divided by five, which is shown as actual input current in table 3.3.

Table 3.3: Current measurement results

Supply current [A]	PLC input voltage (multimeter measurements) [V]	PLC input voltage (PLC measurements) [V]	PLC current measurement of supply current (raw) [a]	PLC current measurement of supply current (divided by five) [A]	Measurement error in percentage [%]
0.7344	0.6420	0.64	3.55	0.71	-3.32
1.819	1.607	1.61	8.94	1.78	-2.14
2.996	2.659	2.66	14.77	2.95	-1.54
5.600	4.963	4.94	27.4	5.50	-1.79
8.46	7.489	7.47	41.47	8.30	-1.89
9.518	8.430	8.45	46.97	9.40	-1.24

3.2.3 Design of power measurement PCB

The power measurement PCB is, as previously addressed designed with a measuring voltage rating of 400V and measuring current rating of 50A. As the current in the circuit is small PCB temperature is not a concern, so the track widths for the primary and secondary side are arbitrarily set to respectively 100 mils and 50 mils. According to Altium Designer’s internal calculator based on the IPC-2221A standard, these track widths can handle respectively 6.45A and 3.90A. While the width is not an issue, the placement and distance to other tracks were a concern with the voltage levels on the PCB. According to table 6-1 in IPC-2221B the distance required between tracks with a voltage of 400VDC or 250VAC is 2.5mm when using external conductors under a height of 3050m above sea level [13]. To ensure all tracks are placed at an appropriately distance from one another, the measuring tool combined with a distance rule are employed in Altium Designer when designing the PCB layout. The LEM element’s schematic model and footprint are obtained from the manufacturer part search library native to Altium Designer. Due to an error with the footprints obtained this way, the pin layout in the footprint for the LV 25-P component was mirrored, and the component had to be placed on the bottom side of the PCB instead of the top as intended. The schematic model and footprint for the RAC20-15DK power supply are obtained from DigiKey [24]. The remaining schematic models and footprints for the PCB terminal blocks and resistors are self-made from the respective datasheets. The final revision of the PCB layout is shown in figure 3.12, while the photos of the finished card with component is shown in figure 3.13.

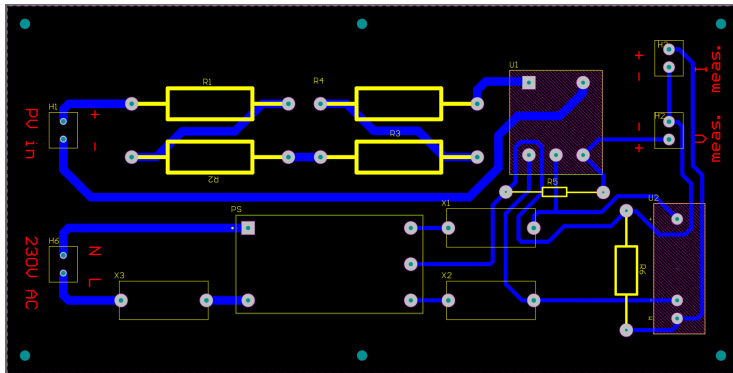


Figure 3.12: Power measurement PCB layout

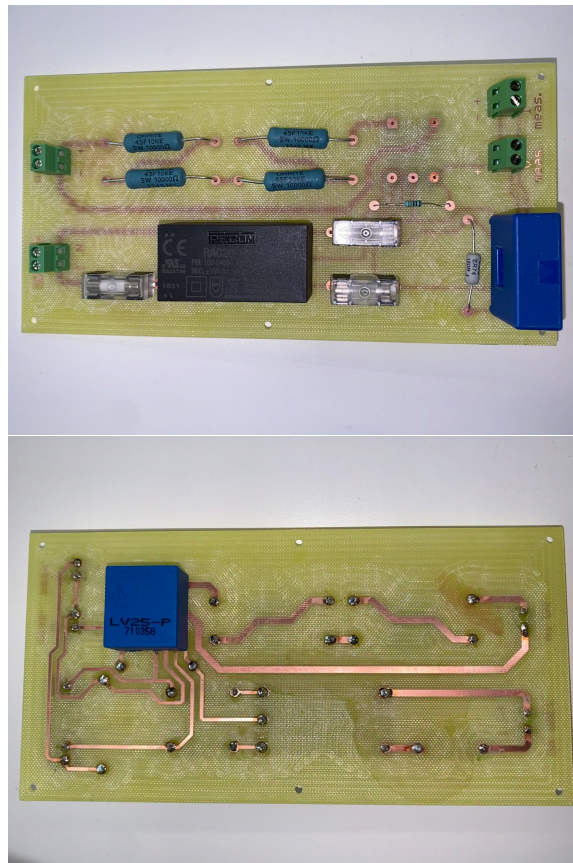


Figure 3.13: Power measurement Complete PCB

3.2.4 Power measurement PCB test

The test of the PCB is conducted in the same manner as the breadboard test, with a maximum test voltage of $\approx 250\text{V}$ and a maximum test current of $\approx 50\text{A}$. equation 3.6, equation 3.7, equation 3.9 and equation 3.8 are used to calculate the voltage, current and error based on PLC data. In difference to the breadboard test, the resistors used on the PCB were measured individually before being soldered on the board. The voltage measuring pre-resistors in series has a resistance of $39.875\text{k}\Omega$, and the measuring resistor has a resistance of 329Ω . The current measuring resistor has a value of 149.1Ω . Due to the raw PLC data fluctuating rapidly within a small area, the value that occurs the most is selected. The results for voltage measurements are shown in table 3.4 while the results for the current measurement are shown in table 3.5.

Table 3.4: Voltage measurement PCB test results

Supply voltage to be measured [V]	PLC input voltage (multimeter measurements) [V]	PLC input voltage (PLC measurements) [V]	PLC voltage measurements of supply voltage [V]	Measurement error in percentage [%]
10.11	0.169	0.166	8.05	-20.38
30.04	0.578	0.581	28.18	-6.19
60.03	1.191	1.191	57.77	-3.76
100.09	2.008	2.010	97.43	-2.66
200.10	4.055	4.061	196.84	-1.63
249.94	5.073	5.077	246.13	-1.52

Table 3.5: Current measurement PCB test results

Supply current [A]	PLC input voltage (multimeter measurements) [V]	PLC input voltage (PLC measurements) [V]	PLC current measurement of supply current (raw) [A]	PLC current measurement of supply current (divided by five) [A]	Measurement error in percentage [%]
0.74	0.533	0.535	3.59	0.72	-2.70
1.83	1.345	1.348	9.04	1.81	-1.09
3.05	2.249	2.259	15.15	3.03	-0.66
5.71	4.223	4.200	28.17	5.63	-1.40
8.59	6.356	6.386	42.83	8.57	-0.23
9.49	7.034	7.021	47.09	9.42	-0.74

3.3 PLC Programming

The PLC code made in this thesis was a modified version of the PLC code made in [4]. The modifications to the code adapts the voltage and current measurement conversions to work correctly with the new PCB, as well as adding a solar position calculator based on time which follows the algorithm from NOAA Global Monitoring Divison [21]. The time used to calculate the sun's position is obtained from the PLC's internal clock which has to be set manually and drifts over time. To fix this, an antenna can be used with the already existing Real Time Clock (RTC) module to obtain time data. The RTC module was not used in this thesis to obtain time data due to a lack of an antenna. The geographical position used in the algorithm is specific to the rig's actual position, and was obtained through Norgeskart [22]. The code was added on top of the code from [4] and implemented to run once the original code has reached it's final state of looping the observe-and-perturb algorithm. The solar position is always calculated but the algorithm switches from observe-and-perturb to solar tracking based on time only when power generated by the solar panels is less than 200W while the wind speed is less than 20m/s and the sun's elevation is above or equal to 10 degrees. This prevents the panel from attempting solar tracking during night time, prevents the program from entering the storm mode and serves its purpose during cloudy weather with fluctuating power generation. Another added functionality is a stand-by mode which is activated when the sun's elevation is below 10 degrees, signifying that the sun cannot be directly seen by the rig. The stand-by mode prevents the rig from doing unnecessary movement when the sun is not visible to reduce power usage. The previous code and thesis do not make it clear which direction is forwards or backwards, so the modified code assumes this based on motor connection color coding, where forward is positive voltage on the red terminal and reverse is opposite polarity. The previous code is also modified to remove unintended behaviour related to IF-statements, but due to time constrains a more comprehensive rewrite is not performed. The unintended behaviour in the previous code includes wrong prioritization in IF-statements for storm mode and misplaced conditions in nested IF-statements. State 0 to state 5 within the code also allows for the rig to enter storm mode directly before the rig's azimuth angle and tilt angle are known. This could result in unintended movement of the rig if the system is initialized during a storm. The new code written during this thesis can be seen in appendix B while the full modified code can be seen in appendix A. Improvements to the code not written due to time constraints includes adding a delay for the time-based solar tracking algorithm to prevent the rig from constantly moving and creating a better visualization program with manual control. Some IF-statements can also have redundant conditions removed to make the code easier to read. The overall flowchart for code produced in this thesis is shown in figure 3.14, where the green states and conditions are added by this thesis.

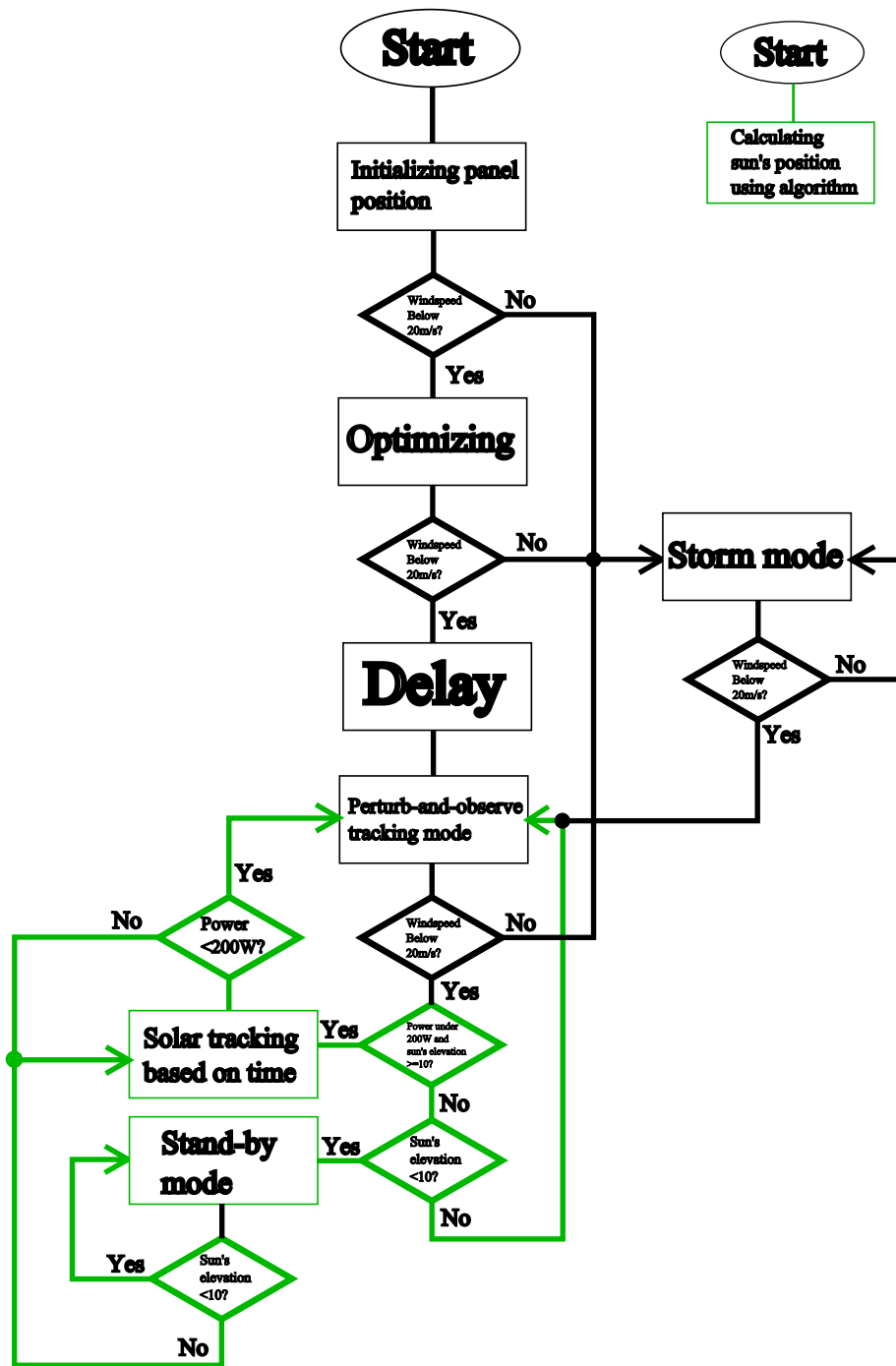


Figure 3.14: Overview flowchart of modified PLC code

3.4 Connection matrix

To allow the connections of the solar panels to be switched between series, parallel and a series-parallel a connection matrix is made. The connection matrix's function is to allow the solar panels' connections to be quickly changed. The design proposed in this thesis uses banana plugs, a terminal block, a diode module, two bus bars and a main switch. Female banana plugs are mounted on a plate made of an isolating material and male banana plugs are used to manually change the connection of the panels. A sketch of the proposed design is shown in figure 3.15.

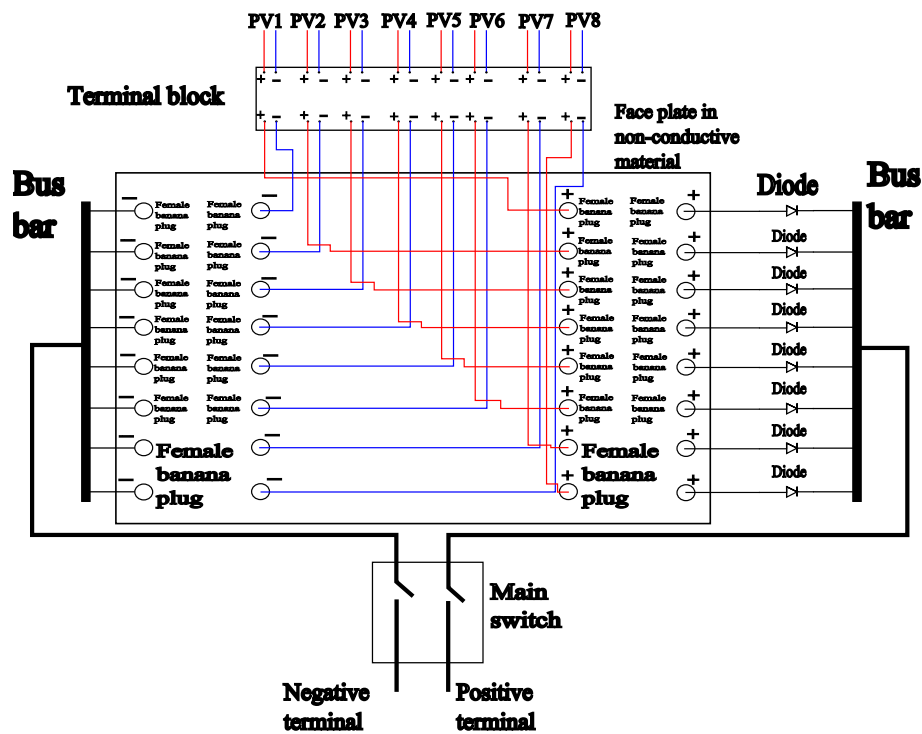


Figure 3.15: Connection matrix design proposal

A terminal block is utilized as an intermediate component to connect the solar panel cables and the cables to the connection matrix. This is done so that the cables to the connection matrix can be removed or replaced without having to anything with the solar panel cables. Eight diodes with a current rating of atleast 6A and a voltage rating of atleast 400V are utilized to prevent reverse power flow when solar panels are connected in parallel. A full parallel connection requires all input and output banana plugs to be used, otherwise the diodes' current rating will be exceeded. The bus bars are used to collect and distribute the power from the solar panels, and need to have a minimum current rating of 50A. The main switch is used to break the flow of power to

the electrical load to allow for safe changes to the connection. A connection example for full series connection in the proposed design is shown in figure 3.16 while a connection example for full parallel operation is proposed in figure 3.17.

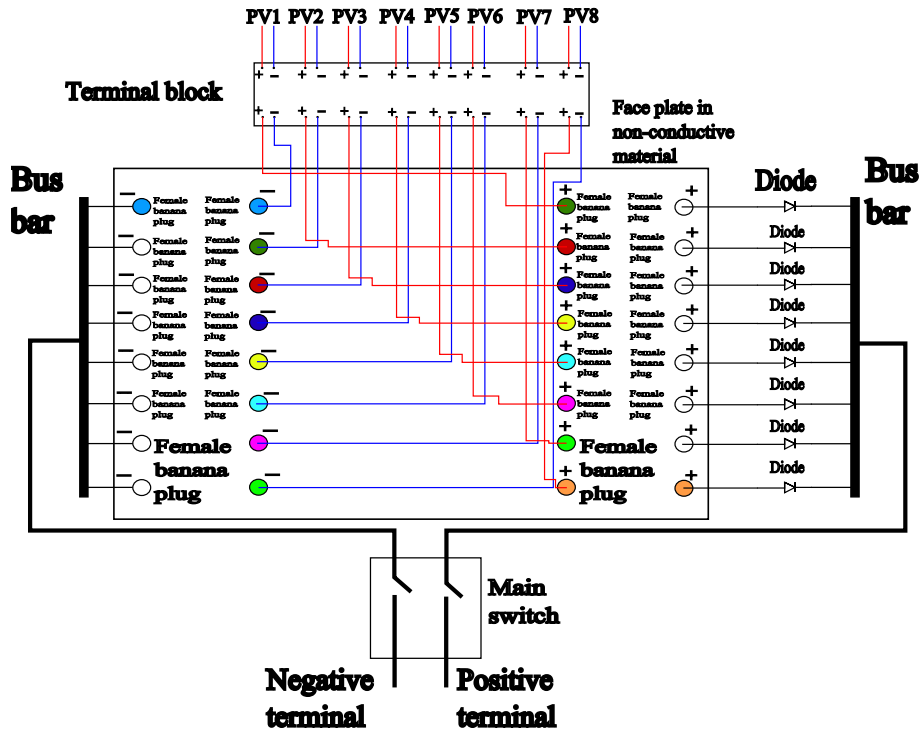


Figure 3.16: Connection matrix full series example

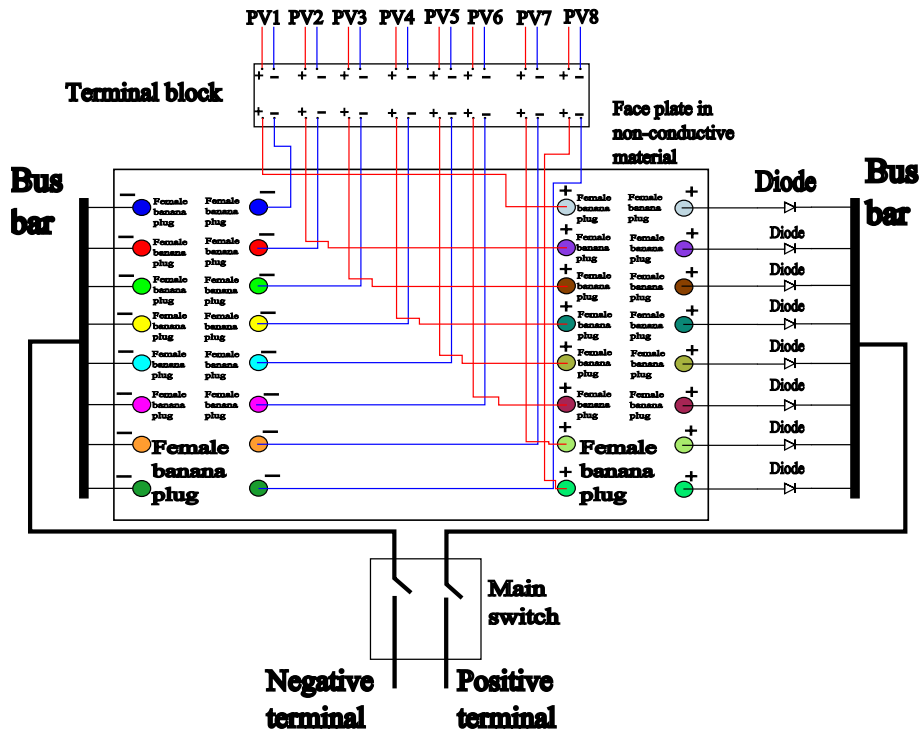


Figure 3.17: Connection matrix full parallel example

The color coding of the female banana plugs corresponds to the connection points of the male banana plugs. The operator must use caution when changing the connections as there will always be voltage present at the female banana plugs and there are no mechanisms to prevent short circuiting the panels.

3.5 Induction sensor holders

The induction sensors' task is to prevent the rig from rotating too far in either azimuth or tilt direction which could lead to damage to either the rig or wiring. There are four sensors in total, two for azimuth direction and two in tilt direction. The sensors have to be mounted in positions where they follow the rotation of the rig and reliably hits and object to detect when having turned the maximum allowed angle. For the azimuth direction the proposed sensor location is mounted on the concrete mast using a steel band around the mast, where they will detect the 24V motor that turns with azimuth angle. As there are several existing ways to do this it was concluded that does not require its own bracket designed. In this location the sensor is easy to mount and will reliably detect the azimuth direction by using the motor housing which does not move up or down. For the tilt direction the proposed sensor location is mounted on top of the rig's motor mount designed in [1] where it will detect the housing

of the azimuth slewing drive at the base of the rig. The bracket which mounts on top of the frame's motor mount is shown in figure 3.18. In this location the sensor will move together with the tilt direction where it will reliably detect the housing once tilt angle reaches its set maximum.

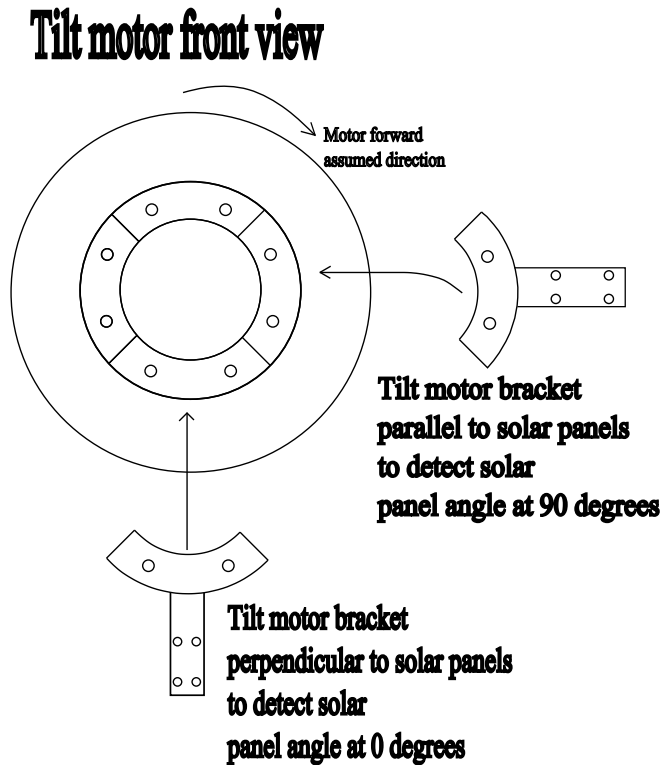


Figure 3.18: Induction tilt sensor bracket design proposal

4 Discussion

4.1 H-bridge

The H-bridge works excellent in both directions on both motor terminals with no noticeable voltage spike when opening the relays. What is not as excellent, however, is the power supply as it supplies too little power. The power supply is an OMRON S8VK-C48024, and it has a maximum power output of 480W with a voltage of 24V and a current of 20A. In the power supply's datasheet it is said that the power supply is unsuited to applications with frequent inrush currents above the rated current [9]. As seen in appendix F the power supply experiences overload every time the motor starts from standstill. The voltage decreases proportionally when the current rises above 20 amperes before rising

again once the current drops. In figure 4.1 the red line marks the power supply's current limit and anything above this results in overloading the power supply. In the experiment shown in the figure the overload state lasts for about 25ms. This issue as well as the current rating of some components means that only one motor can be operated at a time, slowing the optimization time of the algorithm. An experiment was done to check if a large capacitor in parallel with the power supply could remedy the overload during start up, but it was found that the inrush current when charging the capacitor would be too large as well. The proposed solutions for the overload problem would be to either use power electronics to limit current during start up, utilize a power supply with a larger maximum power output or set multiple smaller power supplies in parallel. Another possible issue with the H-bridge could be the temperature when the motors are operating. The track width required for 11 amperes has two different given values depending of if one is following the online calculator based on IPC-2221A or if the IPC-2152 standard is followed. Both values are based on detailed test data and due to a lack of this in-depth testing of the H-bridge there is no basis for determining which is more correct. The motors were operated with no load due to the rig not being completed which resulted in the H-bridge only being tested with a typical current of $<2A$. To properly determine the temperature two tracks with the two different widths should be tested with 11A for an extended period of time before temperature is measured. Yet another issue could be the current rating of the H-bridge. According to an appendix in [4] the motor, as well as a specification sticker on the motor, the motor's no load current is $\leq 5A$, with the rated current being $\leq 11A$ and the peak current being $\leq 35A$ [4]. The actual current when operating the motors is unknown because it is affected by the motor characteristic, the gearing and external load on the rig. As the rated current of the motor is above the 10 ampere current rating of the fuse holder and relays there is a chance that under certain conditions the components may deteriorate over time. This could lead to the fuses breaking when there is no fault, the fuse holders becoming too hot, and the relays becoming hot or ceasing to operate as intended. The solution to this is to replace the fuse holders and relays for ones with a higher current rating. As the relays were reused from a previous thesis, the potential issue was known beforehand in this thesis leading to the fuse holders not having a higher current rating. Depending on the current drawn when the rig is operating, the capacitors might be too small to completely remove the voltage spike. Should the current exceed 10 amperes at any point when the rig is operating, or the capacitors appear to be too small, a new H-bridge design might be warranted.

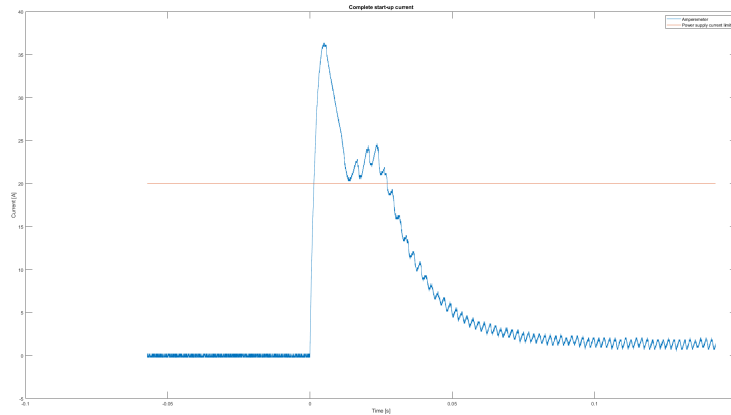


Figure 4.1: Measured motor start-up current, where the blue line is motor current and red is a marker for 20 A

4.2 PLC programming

The PLC code was tested in [4], but needs to be further modified to include blanking times on the H-bridge, as well as testing of the new functions added in this thesis. The different states from [4] original PLC code switches between forward and reverse on the motors depending on their current angle compared to a reference angle. Under certain circumstances the state for one motor may switch from forward to reverse instantly unintended, leading to a possible short circuit of the H-bridge. A short blanking time can be implemented by calling on a function which turns off the motors then waits for a short delay before activating the motor in the correct direction again. It is also unclear how the perturb-and-observe algorithm made in [4] handles local maximums or noise in the power measurements. In [4] it was recommended that the frequency module of the PLC be switched out for an up/down counter instead, as well as rewriting the code to use smaller functions which are called from the main program instead of one large program [4]. In addition to rewriting and testing the original code, the modified code produced in this thesis should be rewritten and tested properly. The code made in this thesis was tested on the PLC to verify solar angle calculations, but due to the rig not being complete the PLC code was not tested with all the rig's components. The code was not tested in combination with any components, and due to issues with simulating the program this was not done either. The testing conducted on the PLC was done by injecting values into the variables and verifying the results by doing the same calculations in MATLAB, on a calculator, as well as using the online solar position calculator found on Global Monitoring Laboratory's website [23]. The algorithm implemented on the PLC appears to give consistent results with it being slightly less accuracy than the same algorithm in MATLAB and the online calculator. In

addition to the lower accuracy, for unknown reasons, to produce the correct result the algorithm requires an extra 180 degrees added to the azimuth angle to produce the same results as the online calculator. The lower accuracy of the PLC code is a result of the algorithm inherently being less accurate than the online calculator, and as a result of the PLC using less significant digits than MATLAB during calculations. In addition to rewriting and optimizing the current code, alternative algorithms may also be implemented and tested before being compared to the perturb-and-observe algorithm.

4.3 Power measurement circuit board

The power measurement card performs well in regards to accuracy and temperature, which was shown during its test. With enough testing and data points the measurement error for different voltage and current levels can be compensated for within the PLC code to obtain more accurate numbers. The PCB was built to be accurate across a wide temperature range with a voltage rating of 400V and current rating 50A, but good accuracy is not critical in regards to the algorithm. The perturb-and-observe algorithm requires a general idea of if the power increases or decreases when perturbing, and the exact value is not of importance. The accuracy of the PCB is more stable in its measuring error than the breadboard test using generic components, but the measuring error with varying temperature was not tested due to low temperature rise during use and a lack of temperature control in the testing facility. Due to the LV 25-P component being placed underneath the card due to an error with the footprint a new PCB may be made for aesthetic or mounting reasons. The safety of the PCB can also be questioned as the solar panel voltage measuring input is not fused in any way to protect against faults. This was not done due to the challenges of achieving this in solar panels as they have a low short circuit current. Another safety concern is the voltage present on the card, which necessitates the PCB being either placed in a closed container or behind a plate to prevent it from being touched. Due to solar panels always generating power when exposed to light, the switch in the connection matrix must be placed in between itself and the power measurement card, or the cables must be disconnected in either the connection matrix or terminal block before allowing any modification to the power measurement card.

4.4 Connection matrix

The proposed solution has not been tested in any capacity, but there are some safety concerns due to the nature of the design. Due to the inherent safety risk of manually changing the connections of the panels with banana plugs a routine has to be made to reduce risk of material damage and human injury. Firstly the main switch has to be turned off before disconnecting the banana plugs otherwise arcing may appear. Secondly the operator has to be wary of electrical shock as the solar panels cannot be disconnected with the switch in this configuration. Thirdly, the connection matrix must be locked and inaccessible to anyone not

qualified to operate it. Over each panel there is only maximum 44.5V combined with isolated banana plugs makes this a viable design safety wise with some stipulations. The design could also be done differently by replacing the main switch with one or several two pole multi-channel switches to either break the flow of power for each separate solar panel or change their connection directly within the switch. The switch could also control several contactors to change the connections of the solar panels. Using one of these designs instead of the current proposed one would remove the need for manual connections with banana plugs while improving the safety at the loss of connection options.

4.5 Induction sensor holders

The proposed positions have not been tested in any capacity, but the positions are expected to work. A consideration which was not done is the stability of the brackets under movement and external load on the brackets which could offset the angle at which the sensors detects obstacles. The azimuth sensors must also be placed precisely on the concrete mast to allow the rig to have the needed movement to follow the sun. The angle the azimuth sensors sit at compared to geographical north must also be found to allow the rig to accurately use the solar position algorithm. Currently the PLC code arbitrarily sets the angle to 15 degrees once the induction sensor detects something which must be changed once the actual position is determined. The tilt sensors angle does not need to be changed as long as the bracket's angle is correct and the angle is held stable during movement and external load. The tilt sensors are set to only allow the rig to tilts between 0 degrees and 90 degrees instead of ± 90 degrees. This could lead to an increase in azimuth movement of the rig when the sun's position is behind the panels and the tilt angle is not allowed to move into negative angles.

5 Conclusion

The H-bridge PCB functioned as intended and allows for bidirectional movement of both motors with the limitation of one motor running at a time. The power supply purchased for the motors provides too little power when starting a motor from standstill, which has to be addressed. Due to unknown current drawn from the motors when the entire rig is installed a new PCB may have to be made if the current exceeds 10 amperes. The proposed solutions for this is to buy a power supply with higher power rating, place another identical power supply in parallel with the current one, or use a current limiting circuit during start. The power measurement PCB provided accurate measurements of current, and a slightly less accurate voltage measurements. The PCB measures voltage up to 400V and currents up to 50A and was tested on voltages up to 250V and currents up to 50A with good results. The PLC code created in this thesis is a modified revision of the code in [4]. The PLC code should be rewritten either completely or partly and the new functionalities should be tested properly. The induction sensor bracket design has been sketched and their locations proposed.

They have not been modeled, made, or tested, but the positions are believed to work for the intended purpose. The connection matrix has had its design sketched, its components mostly picked out and its safety discussed. Other possible designs have been proposed instead of the main one, but they have not been discussed in the same amount of detail. The connection matrix is not made nor tested, but it is believed to function as intended with a satisfying degree of safety regarding its operation.

5.1 Further work

Future work that should be done is presented in the list below. The PLC code should have some parts rewritten to improve it and have the new functionalities tested before it can be used properly. Optionally the H-bridge PCB can also be redesigned with larger capacitors and components which have a higher current rating. Optionally as well, the power measurement circuit board can be redesigned to allow all components to be mounted on one side.

- Fix the power supply issue for the H-bridge.
- Model and create brackets for the induction sensors.
- Create and install the connection matrix.
- Find a suitable position and create a bracket for the pyranometer.
- According to [4] the frequency module for the PLC is recommended to be replaced with an up-down counter instead.
- Also according to [4] a mechanical safety mechanism should be created to sever the motor cables in case of issues with either the PLC program or induction sensors.
- Obtain time data for the PLC using the RTC module instead of the internal clock.
- Manual control of the rig should be implemented for safety and research purposes.
- Rewrite, test and optimize parts of the PLC code.
- Install the rig and connect everything.
- Test the performance of the optimization algorithm.

References

- [1] H. Limstrand & T. Juell, “*Konstruksjon av to-akset solcellerigg med retningsstyring*”, Bachelor thesis, Department of Technology, UiT The Arctic University of Norway, Narvik, 2016.
- [2] “LEM International SA. *Current Transducer LA 55-P*”. 6th of July, 2023. Available: https://www.lem.com/sites/default/files/products_datasheets/la_55-p_v19.pdf. Accessed on: 10.05.2024.
- [3] “LEM International SA. *Voltage Transducer LV 25-P*”. 28th of December, 2022. Available: https://www.lem.com/sites/default/files/products_datasheets/lv_25-p_v21.pdf. Accessed on: 10.05.2024.
- [4] E. Haque, “*Solar Angle Optimizer*”, Master thesis, Department of Electrical Engineering, UiT The Arctic University of Norway, Narvik, 2023.
- [5] M. R. Skjelbred, “*Solar Angle Optimizer*”, Master thesis, Department of Electrical Engineering, UiT The Arctic University of Norway, Narvik, 2022.
- [6] RS PRO. “*RS PRO CB Series Epoxy-coated Solid Electrolytic Tantalum Capacitor*”. No date. Available: <https://docs.rs-online.com/c60f/0900766b816c111d.pdf>. Accessed on: 10.05.2024.
- [7] RS PRO. “*RS Pro 5mm Pitch Straight PCB Terminal Block with Screw Termination, Through Hole, 2 Way*”. No date. Available: <https://docs.rs-online.com/e2b9/0900766b8157c82b.pdf>. Accessed on: 10.05.2024.
- [8] SCHURTER. “*Fuseholder Open Design, 5 x 20 mm, THT, var. Covers, IEC 60335-1*”. 22th of July, 2014. Available: <https://docs.rs-online.com/cc1f/0900766b814209b6.pdf>. Accessed on: 10.05.2024.
- [9] OMRON Corporation. “*Switch Mode Power Supply S8VK-C (60/120/240/480-W Models)*”. No date. Available: https://assets.omron.eu/downloads/latest/datasheet/en/t058_s8vk-c_switch_mode_power_supply_datasheet_en.pdf?v=10. Accessed on 10.05.2024.
- [10] *Standard for Determining Current Carrying Capacity in Printed Board Design*. IPC-2152, IPC, Bannockburn, Illinois, USA, August 2009.
- [11] Z. Peterson, “*IPC-2221 Calculator for PCB Trace Current and Heating*”. 26th of September, 2023. Available: <https://resources.altium.com/p/ipc-2221-calculator-pcb-trace-current-and-heating>. Accessed on: 10.05.2024.
- [12] *Elektriske lavspenningsinstallasjoner*, NEK 400:2022, Norsk elektroteknisk komite, No location, 2022.

- [13] *Generic Standard on Printed Board Design*, IPC-2221B, IPC, Bannockburn, Illinois, USA, November 2012.
- [14] Rapidonline. “*Hongfa HF140FF/024-2HTF PCB Relay 24VDC 2 x SPST-NO 10A*”. No date. Available: <https://www.rapidonline.com/hongfa-hf140ff-024-2htf-pcb-relay-24vdc-2-x-spst-no-10a-71-4634>. Accessed on: 10.05.2024.
- [15] RECOM. “*RAC20-K*”. November, 2023. Available: <https://g.recomcdn.com/media/Datasheet/pdf/.fg2aXvY/.t4c211b3c4016d66c96f6/Datasheet-132/RAC20-K.pdf>. Accessed on: 10.05.2024.
- [16] Tyco Electronics. “*High Power Resistors - Type ER/ERV Series*”. November, 2008. Available: <https://docs.rs-online.com/fa28/A700000006727782.pdf>. Accessed on: 10.05.2024.
- [17] TE connectivity. “*Metal Film Fixed Resistors - Type LR Series*”. July, 2011. Available: <https://docs.rs-online.com/5bd5/0900766b81560e40.pdf>. Accessed on: 10.05.2024.
- [18] OHMITE. “*40 Series - Ohmicone® Silicone-Ceramic Conformal Axial Terminal Wirewound 1% and 5% Tolerance Standard*”. No date. Available: <https://docs.rs-online.com/c1ed/0900766b8154da78.pdf>. Accessed on: 10.05.2024.
- [19] Phoenix contact. “*PCB terminal block - MKDSN 2,5/ 2 - 1890963*”. 4th of June, 2015. Available: <https://docs.rs-online.com/5783/0900766b812bfb1e.pdf>. Accessed on: 10.05.2024.
- [20] WAGO. “*Product Manual 4-channel, 0-10VDC, Single-ended*”. WAGO. No Date. Available: www.wago.com/global/d/467. Accessed on: 10.05.2024.
- [21] NOAA Global Monitoring Divison. “*General Solar Position Calculations*”. No date. Available: <https://gml.noaa.gov/grad/solcalc/solareqns.PDF>. Accessed on: 10.05.2024.
- [22] Kartverket. “*Norgeskart*”. No date. Available: Norgeskart.no. Accessed on: 10.05.2024.
- [23] NOAA Global Monitoring divison. “*NOAA Solar Calculator*”. No date. Available: <https://gml.noaa.gov/grad/solcalc/>. Accessed on: 12.05.2024.
- [24] Digikey. “*RAC20-15DK Footprints and Models*”. No date. Available: <https://www.digikey.no/en/models/9644722>. Accessed on: 10.05.2024.

A Full modified PLC code

```
1 PROGRAM PLC_PRG
2 VAR
3     CL1,CL2: DWORD;
4     State1 ,State2 ,Pstate1 ,Pstate2 : DWORD:=0;
5     J,X,H,Counter1 ,Counter2: REAL:=0;
6     WindSpeed ,IS1 ,IS2 , IS3 , IS4: REAL;
7     Irrad ,AM, PM: REAL;
8     AziDeg ,TltDeg ,Deg1 ,Deg2 ,RefDeg :REAL:=0;
9     Delay :TON;
10    Time_And_Date:typWagoTimeComponents;
11    Voltage_Rm , Voltage_Pre_Resistor_Rm ,Current_Rm :
        REAL:=0;
12    Voltage_LEM_Voltage , Current_LEM_Voltage:REAL;
13    pi:REAL := 3.14159265359;
14    time_zone:INT;
15    longitude_rad:REAL := 0.30431; longitude_deg:REAL
        := longitude_rad*(360/(2*pi));
16    latitude_rad:REAL := 1.1944; latitude_deg:REAL:=
        latitude_rad*(360/(2*pi));
17    y,eqtime ,decl_rad ,decl_deg ,time_offset ,tst ,ha_rad
        ,ha_deg ,zenith_rad ,zenith_deg: REAL := 0;
18    theta_rad ,theta_deg ,sun_elevation ,sun_azimuth: REAL
        := 0;
19    day_of_year ,days_in_year ,day ,month ,hour ,minute ,
        second:UINT := 0;
20    Z,I ,Power ,P0,P1,P2,P3,P4,P5:REAL:=0;
21    M1FWD, M1_REV: BOOL:=FALSE;
22    M2FWD, M2_REV: BOOL:=FALSE;
23    LStorm ,LOAzi ,LOTlt ,LHAzi ,LHTlt:BOOL:=FALSE;
24    Storm:BOOL;
25    Voltage_measured , Raw_Voltage_Input ,
        Raw_Current_Input , Current_measured: REAL;
26    Pmax, P2Max: REAL;
27    FbDatalogger1:FbDatalogger;
28    xActivate:BOOL:=TRUE;
29    aValues:ARRAY[1..MAX_CHANNELS] OF REAL;
30    xEvent:BOOL;
31    log_xReady:BOOL;
32    log_sStatus: STRING;
33    log_oStatus : WagoSysErrorBase .
        FbResult;
34    typConfigParameters:typConfigdatalogger;
35    xInit:BOOL:=TRUE;
```

36 END_VAR

37

```
38     typConfigParameters.bDatalogger_type:=3; //
        Dataplotter format
39     typConfigParameters.sPath := '/media/sd/'; //Path
40     typConfigParameters.sFilename := 'PLC_Logfile.csv
        ';
41     typConfigParameters.xCyclicLogging:=TRUE;
42     typConfigParameters.bInterval :=3; //Interval
43     typConfigParameters.uiIntervalFactor:=2; // write
        every 2 seconds
44     //Channel Configuration
45     typConfigParameters.atypChannelConfig[1].
        xChannelExists:=TRUE;
46     typConfigParameters.atypChannelConfig[1].
        sChannelName:= 'Raw-Voltage-Input';
47     typConfigParameters.atypChannelConfig[2].
        xChannelExists:=TRUE;
48     typConfigParameters.atypChannelConfig[2].
        sChannelName:= 'Raw-Current-Input';
49     typConfigParameters.atypChannelConfig[3].
        xChannelExists:=TRUE;
50     typConfigParameters.atypChannelConfig[3].
        sChannelName:= 'Measured-Voltage-Input';
51     typConfigParameters.atypChannelConfig[4].
        xChannelExists:=TRUE;
52     typConfigParameters.atypChannelConfig[4].
        sChannelName:= 'Measured-Current-Input';
53     aValues[1]:= Raw_Voltage_Input;
54     aValues[2]:= Raw_Current_Input;
55     aValues[3]:= Voltage_measured;
56     aValues[4]:= Current_measured;
57     FbDatalogger1(
58         xActivate:=xActivate ,
59         aValues:=aValues ,
60         xEvent:=xEvent ,
61         typConfigParameters:=typConfigParameters ,
62         oStatus=> log_oStatus ,
63         sStatus=> log_sStatus ,
64         xReady=> log_xReady );
65     //Sensors configuration
66     PM:= IoConfig_Globals.Mapping.PM; //Pyranometer
67     AM:= IoConfig_Globals.Mapping.AM; //Anemometer
68     IS1:=IoConfig_Globals.Mapping.IS1; //4 Induction sensors
69     IS2:=IoConfig_Globals.Mapping.IS2;
```

```

70 IS3:=IoConfig_Globals_Mapping.IS3;
71 IS4:=IoConfig_Globals_Mapping.IS4;
72 CL1:= IoConfig_Globals_Mapping.CL1; //2 pulse counter for
      motor positioning
73 CL2:= IoConfig_Globals_Mapping.CL2;
74 //(Input/32760)*10 is Wago 750-468 data to voltage
      conversion (see manual).
75 Windspeed:= (AM/32760)*10*0.164; //Sensitivity of
      anemometer is 0.165 Vs/m
76 //WindSpeed:=AM*SFV*6.0975; //Sensitivity of Anemometer
      is 0.164 Vs/m. Old code from Haque's thesis
77 Irrad:=- (PM/32760)*10*49.5; //Sensitivity of Pyranometer
      is 49.5 mV*m^2/W
78 //Irrad:=(SFV*PM)/49.5; //Sensitivity of Pyranometer is
      49.5. Old code from Haque's thesis
79 //Raw input data for voltage and current
80 Raw_Voltage_Input:= IoConfig_Globals_Mapping.Voltage;
81 Raw_Current_Input:= IoConfig_Globals_Mapping.Current;
82 //Calculating input voltage and current
83 Voltage_Rm:= 329; //Measured value using multimeter
84 Voltage_Pre_Resistor_Rm:= 39875; //Measured value using
      multimeter
85 Voltage_LEM_Voltage := (Raw_Voltage_Input/32760)*10; //
      Value of 32760 corresponds to 10V input (found in
      module manual), multiply by 10 because it measures
      +-10V.
86 Voltage_measured:= (Voltage_LEM_Voltage/Voltage_Rm)*0.4*
      Voltage_Pre_Resistor_Rm; // 0.4 is 1000/2500 (LEM
      Element turns ratio reversed) because PLC seemingly
      cannot calculate it otherwise
87 Current_Rm:= 149.1; //Measured value using multimeter
88 Current_LEM_Voltage := (Raw_Current_Input/32760)*10; //
      Value of 32760 corresponds to 10V input (found in
      module manual), multiply by 10 because it measures
      +-10V.
89 Current_measured:= (Current_LEM_Voltage/Current_Rm)
      *(1000/1); //1000/1 is LEM Element turns ratio
      reversed
90 Power:= Voltage_measured*Current_measured;
91 State1 := CL1;
92 IF State1<>Pstate1 THEN
93     Counter1:= Counter1+1;
94     //ELSE Counter1:= Counter1;
95 END IF
96 Pstate1:=State1;
97 IF M1_REV=TRUE THEN Deg1:= 0.05037287*Counter1;

```

```

98  ELSIF MLFWD= TRUE THEN Deg1:= 0.05137287*Counter1;
      END_IF
99  State2 := CL2;
100 IF State2<>Pstate2 THEN
101      Counter2:= Counter2+1;
102      //ELSE Counter2:= Counter2;
103  END_IF
104  Pstate2:=State2;
105  Deg2:= 0.05337287*Counter2;
106  //For Visualisation
107  IF I>-1 AND I<5 THEN LOAzi:= TRUE; ELSE LOAzi:=FALSE;
      END_IF
108  IF I>4 AND I<10 THEN LOTlt:= TRUE; ELSE LOTlt:=FALSE;
      END_IF
109  IF I>9 AND I<12 THEN LHAzi:= TRUE; ELSE LHAzi:=FALSE;
      END_IF
110  IF I>11 AND I<14 THEN LHTlt:= TRUE; ELSE LHTlt:=FALSE;
      END_IF
111  //Calculation of solar position
112  time_zone := 1; //Timezone set to CET always at request
      of supervisor
113  //time_zone := Time_And_Date.TimeZone.iOffset/60; //
      Variable timezone (auto-switch between CET AND CEST)
114  Time_And_Date:= WagoAppTime.FuGetLocalTimeComponents();
      // Puts time and date data into the Time_And_Date
      struct
115  month := Time_And_Date.uiMonth;
116  day := Time_And_Date.uiDay;
117  hour := Time_And_Date.uiHour;
118  minute := Time_And_Date.uiMinute;
119  second := Time_And_Date.uiSecond;
120  day_of_year := Time_And_Date.uiYday;
121  IF WagoAppTime.FuIsLeapYear(Time_And_Date.uiYear) THEN //
      Checks for leap year, relevant to calculation
      algorithm
122      days_in_year:= 366;
123  ELSE
124      days_in_year:=365;
125  END_IF
126  y := (2*pi/days_in_year)*(day_of_year - 1 +((hour-12)/24)
      );
127  eqtime := 229.18*(0.000075 + (0.001868*COS(y)) -
      (0.032077*SIN(y)) - (0.014615*COS(2*y)) - (0.040849*
      SIN(2*y)));
128  decl_rad := 0.006918 - 0.399912*COS(y) + 0.070257*SIN(y)
      - 0.006758*COS(2*y) + 0.000907*SIN(2*y)

```



```

129 - 0.002697*COS(3*y) + 0.00148*SIN (3*y);
130 decl_deg := decl_rad * (360/(2*pi));
131 time_offset := eqtime + (4*longitude_deg) - (60*time_zone
    );
132 tst := (hour*60) + minute + (second/60) + time_offset;
133 ha_deg := (tst/4) - 180;
134 ha_rad := ha_deg * ((2*pi)/360);
135 zenith_rad := ACOS((SIN(latitude_rad)*SIN(decl_rad)) + (
    COS(latitude_rad)*COS(decl_rad)*COS(ha_rad)));
136 theta_rad := -ACOS(-((SIN(latitude_rad)*COS(zenith_rad)-
    SIN(decl_rad))/(COS(latitude_rad)*SIN(zenith_rad)))+
    pi);
137 theta_deg := theta_rad * (360/(2*pi));
138 sun_elevation := 90 - (zenith_rad*(360/(2*pi)));
139 sun_azimuth := theta_deg+180;
140 //STORM MODE
141 //IF WindSpeed>20 THEN I:=100; Delay(IN:=FALSE); END_IF
    // Original code from Haque's thesis
142 //Every state already has a check for windspeed, having
    multiple if-statements set the state independently
    could lead to unforeseen trouble
143 IF I=100 AND X=0 THEN LStorm:=TRUE; M1FWD:=FALSE;
    M1REV:=FALSE; M2FWD:=FALSE; M2REV:=FALSE; Counter2
    :=0; Deg2:=0; RefDeg:=TltDeg; X:=1; Delay(IN:=FALSE);
144 ELSIF I=100 AND X=1 AND IS4>32766 AND Deg2<(80-RefDeg)
    THEN M2REV:=FALSE; M2FWD:=TRUE;
145 ELSIF I=100 AND X=1 AND IS4>32766 AND Deg2>(80-RefDeg)
    THEN M2REV:=FALSE; M2FWD:=FALSE; Delay(IN:=TRUE
    , PT:=T#30S); IF NOT(Delay.Q) THEN RETURN;
146 TltDeg:=TltDeg+Deg2; Counter2:=0; Deg2:=0; X:=0;
    J:=2; LStorm:=FALSE; I:=150;
147 END_IF Delay(IN:=FALSE);
148 END_IF
149 IF WindSpeed<20 AND J=2 AND IS3>32766 AND (TltDeg-RefDeg
    )>Deg2 THEN M2FWD:=FALSE; M2REV:=TRUE;
150 ELSIF WindSpeed<20 AND J=2 AND IS3>32766 AND (TltDeg-
    RefDeg)<Deg2 THEN M2FWD:=FALSE; M2REV:=
    FALSE; TltDeg:=TltDeg-Deg2; Counter2:=0; Deg2:=0; I
    :=10; J:=0;
151 END_IF
152 //SOLAR TRACKING MODE BASED ON TIME
153 // Enters solar tracking mode from state 13
154 IF I=201 AND Power<200 AND Windspeed<20 AND sun_elevation
    >=10 THEN
155 IF (sun_azimuth-1)<AziDeg AND AziDeg<(sun_azimuth
    +1) THEN M1FWD:=FALSE; M1REV:=FALSE; I:=202; // -1

```

```

degree-around-actual
156 ----- ELSIF AziDeg < sun_azimuth THEN M1FWD:=TRUE;
M1.REV:=FALSE; -//sun-azimuthal-angle-where-it-doesn't
move to prevent
157     ELSIF AziDeg > sun_azimuth THEN M1FWD:=FALSE;
M1.REV:=TRUE; // the rig from constantly
moving back and forth
158     END_IF
159 ELSIF I=202 AND Power<200 AND Windspeed<20 AND
sun_elevation >=10 THEN
160     IF (sun_elevation-1)<TltDeg AND TltDeg<(
sun_elevation+1) THEN M2FWD:=FALSE; M2.REV:=
FALSE;
161     ELSIF TltDeg < sun_elevation THEN M2FWD:=TRUE;
M2.REV:=FALSE;
162     ELSIF TltDeg > sun_elevation THEN M2FWD:=FALSE;
M2.REV:=TRUE;
163     END_IF
164 ELSIF (I=201 OR I=202) AND Power>=200 THEN
165     M1FWD:=FALSE; M1.REV:=FALSE; M2FWD:=FALSE;
M2.REV:=FALSE; I:=10;
166 END_IF
167 //STAND-BY MODE WHEN SUN IS DOWN
168 //Enters stand-by mode from state 13
169 IF I=300 THEN M1FWD:=FALSE; M1.REV:=FALSE; M2FWD:=FALSE
; M2.REV:=FALSE;
170 ELSIF I=300 AND sun_elevation >=10 THEN I:=201;
171 END_IF
172 //State 0
173 //IF Windspeed>20 THEN I:=100; //Moved from bottom of IF-
statement due to Structured Text prioritization. Also
removed due to azimuth and tilt angles being unknown
at this state.
174 IF IS1>32766 AND I=0 AND WindSpeed<20 THEN
175     IF I=0 AND Z=0 THEN P0:= Power; Z:=1;
176     ELSIF I=0 AND Z=1 AND Deg1<3 THEN M1FWD:= FALSE;
M1.REV:= TRUE; P1:=Power;
177     ELSIF I=0 AND Z=1 AND Deg1>3 THEN M1FWD:= FALSE;
M1.REV:= FALSE; AziDeg:=AziDeg-Deg1; I:=1;
178     END_IF
179 END_IF
180 //State 1
181 //IF WindSpeed>20 THEN I:=100; //Moved from bottom of IF-
statement due to Structured Text prioritization. Also
removed due to azimuth and tilt angles being unknown
at this state.

```

```

182 IF IS2>32766 AND I=1 AND WindSpeed<20 AND P1>P0 THEN
      Counter1:=0; Deg1:=0; I:=0; Z:=0;
183 ELSIF IS2>32766 AND I=1 AND WindSpeed<20 AND P1=P0 THEN
      Counter1:=0; Deg1:=0; I:=0; Z:=0;
184 ELSIF IS2>32766 AND I=1 AND WindSpeed<20 AND P0>P1 THEN
      Counter1:=0; Deg1:=0; I:=2; Z:=0;
185 END_IF
186 //State 2
187 //IF Windspeed>20 THEN I:=100; //Moved from bottom of IF-
      statement due to Structured Text prioritization. Also
      removed due to azimuth and tilt angles being unknown
      at this state.
188 IF IS1>32766 AND I=2 AND WindSpeed<20 THEN
189     IF I=2 AND Z=0 THEN P0:= Power; Z:=1;
190     ELSIF I=2 AND Z=1 AND Deg1<3 THEN M1REV:= FALSE;
      M1FWD:= TRUE; P1:=Power;
191     ELSIF I=2 AND Z=1 AND Deg1>3 THEN M1FWD:= FALSE;
      M1REV:= FALSE; AziDeg:=AziDeg+Deg1; I:=3;
      Counter1:=0; Deg1:=0;
192     END_IF
193 END_IF
194 //State3
195 //IF WindSpeed>20 THEN I:=100; //Moved from bottom of IF-
      statement due to Structured Text prioritization. Also
      removed due to azimuth and tilt angles being unknown
      at this state.
196 IF IS2>32766 AND I=3 AND WindSpeed<20 AND P1>P0 THEN I
      :=2; Z:=0;
197 ELSIF IS2>32766 AND I=3 AND WindSpeed<20 AND P1=P0 THEN
      I:=2; Z:=0;
198 ELSIF IS2>32766 AND I=3 AND WindSpeed<20 AND P0>P1 THEN
      I:=4; Z:=0;
199 END_IF
200 //State4
201 IF IS2>32766 AND I=4 AND WindSpeed<20 AND Deg1<3 THEN
      M1FWD:= FALSE; M1REV:= TRUE;
202 ELSIF IS2>32766 AND I=4 AND WindSpeed<20 AND Deg1>3 THEN
      M1FWD:= FALSE; M1REV:= FALSE; AziDeg:=AziDeg-Deg1;
      I:=5; Counter1:=0; Deg1:=0;
203 END_IF
204 //State 5
205 //IF Windspeed>20 THEN I:=100; //Moved from bottom of IF-
      statement due to Structured Text prioritization. Also
      removed due to azimuth and tilt angles being unknown
      at this state.
206 IF IS3>32766 AND I=5 AND WindSpeed<20 THEN

```

```

207     IF I=5 AND Z=0 THEN P0:= Power; Z:=1;
208     ELSIF I=5 AND Z=1 AND Deg2<3 THEN M2FWD:= FALSE;
        M2.REV:= TRUE; P1:=Power;
209     ELSIF I=5 AND Z=1 AND Deg2>3 THEN M2FWD:= FALSE;
        M2.REV:= FALSE; TltDeg:=TltDeg-Deg2; I:=6;
210     END_IF
211 END_IF
212 //State 6
213 IF WindSpeed>20 THEN I:=100; //Moved from bottom of IF-
        statement due to Structured Text prioritization
214 ELSIF IS3>32766 AND I=6 AND WindSpeed<20 AND P1>P0 THEN
        Counter2:=0; Deg2:=0; I:=5; Z:=0;
215 ELSIF IS3>32766 AND I=6 AND WindSpeed<20 AND P1=P0 THEN
        Counter2:=0; Deg2:=0; I:=5; Z:=0;
216 ELSIF IS3>32766 AND I=6 AND WindSpeed<20 AND P0>P1 THEN
        Counter2:=0; Deg2:=0; I:=7; Z:=0;
217 END_IF
218 //State 7
219 IF Windspeed>20 THEN I:=100; //Moved from bottom of IF-
        statement due to Structured Text prioritization
220 ELSIF IS3>32766 AND I=7 AND WindSpeed<20 THEN
221     IF I=7 AND Z=0 THEN P0:= Power; Z:=1;
222     ELSIF I=7 AND Z=1 AND Deg2<3 THEN M2.REV:= FALSE;
        M2FWD:= TRUE; P1:=Power;
223     ELSIF I=7 AND Z=1 AND Deg2>3 THEN M2FWD:= FALSE;
        M2.REV:= FALSE; TltDeg:=TltDeg+Deg2; I:=8;
        Counter2:=0; Deg2:=0;
224     END_IF
225 END_IF
226 //State8
227 IF WindSpeed>20 THEN I:=100; //Moved from bottom of IF-
        statement due to Structured Text prioritization
228 ELSIF IS4>32766 AND I=8 AND WindSpeed<20 AND P1>P0 THEN
        I:=7; Z:=0;
229 ELSIF IS4>32766 AND I=8 AND WindSpeed<20 AND P1=P0 THEN
        I:=7; Z:=0;
230 ELSIF IS4>32766 AND I=8 AND WindSpeed<20 AND P0>P1 THEN
        I:=9; Z:=0;
231 END_IF
232 //State9
233 IF WindSpeed>20 THEN I:=100; //Moved from bottom of IF-
        statement due to Structured Text prioritization
234 ELSIF IS4>32766 AND I=9 AND WindSpeed<20 AND Deg2<3 THEN
        M2FWD:= FALSE; M2.REV:= TRUE;
235 ELSIF IS4>32766 AND I=9 AND WindSpeed<20 AND Deg2>3 THEN
        M2FWD:= FALSE; M2.REV:= FALSE; Delay(IN:=TRUE, PT:=

```

```

T#60S); IF NOT(Delay.Q) THEN RETURN; END_IF Delay(IN:=
FALSE); I:=10; TltDeg:=TltDeg-Deg2; Counter2
:=0; Deg2:=0;
236 END_IF
237 //Tracking M1
238 IF WindSpeed>20 THEN I:=100; //Moved from bottom of IF-
statement due to Structured Text prioritization
239 ELSIF I=10 AND WindSpeed<20 THEN
240 IF I=10 AND H=0 AND Deg1<1 THEN P0:= Power; H:=1;
241 ELSIF I=10 AND H=1 AND Deg1<3 AND IS1>32766 AND
IS2>32766 AND WindSpeed<20 THEN M1.REV:= FALSE
; M1.FWD:= TRUE; P1:= Power;
242 ELSIF I=10 AND H=1 AND Deg1>3 AND IS1>32766 AND
IS3>32766 AND WindSpeed<20 THEN M1.REV:= FALSE
; M1.FWD:= FALSE; AziDeg:=AziDeg+Deg1; H:=2;
Counter1:=0; Deg1:=0;
243 ELSIF I=10 AND H=2 AND Deg1<6 AND IS1>32766 AND
IS2>32766 AND WindSpeed<20 THEN M1.FWD:= FALSE
; M1.REV:= TRUE; P2:=Power;
244 ELSIF I=10 AND H=2 AND Deg1>6 AND WindSpeed<20
THEN M1.FWD:= FALSE; M1.REV:= FALSE; AziDeg:=
AziDeg-Deg1; I:=11; H:=0; Counter1:=0; Deg1
:=0;
245 END_IF;
246 P2Max:= MAX(P0,(MAX(P1,P2)));
247 END_IF
248 IF WindSpeed>20 THEN I:=100; //Moved from bottom of IF-
statement due to Structured Text prioritization
249 ELSIF I=11 AND P2Max=P2 AND WindSpeed<20 THEN M1.FWD:=
FALSE; M1.REV:= FALSE; P0:=0; P1:=0; P2:=0; P3:=0;
Counter1:=0; Deg1:=0; I:=12;
250 ELSIF I=11 AND P2Max = P0 AND WindSpeed<20 AND Deg1<3
THEN M1.REV:= FALSE; M1.FWD:= TRUE;
251 ELSIF I=11 AND P2Max = P0 AND WindSpeed<20 AND Deg1>3
THEN M1.REV:= FALSE; M1.FWD:= FALSE; AziDeg:=AziDeg+
Deg1; P0:=0; P1:=0; P2:=0; P3:=0; Counter1:=0; Deg1
:=0; I:=12;
252 ELSIF I=11 AND P2Max= P1 AND WindSpeed<20 AND Deg1<6 THEN
M1.REV:= FALSE; M1.FWD:= TRUE;
253 ELSIF I=11 AND P2Max= P1 AND WindSpeed<20 AND Deg1>6 THEN
M1.REV:= FALSE; M1.FWD:= FALSE; AziDeg:=AziDeg+Deg1;
P0:=0; P1:=0; P2:=0; P3:=0; Counter1:=0; Deg1:=0; I
:=12;
254 END_IF
255 //Tracking M2
256 IF WindSpeed>20 THEN I:=100; //Moved from bottom of IF-

```

```

statement due to Structured Text prioritization
257 ELSIF I=12 AND WindSpeed<20 THEN
258     IF I=12 AND H=0 AND Deg2<1 THEN P0:= Power; H:=1;
259     ELSIF I=12 AND H=1 AND Deg2<3 AND IS3>32766 AND
        IS4>32766 AND WindSpeed<20 THEN M2.REV:= FALSE
        ; M2FWD:= TRUE; P1:= Power;
260     ELSIF I=12 AND H=1 AND Deg2>3 AND IS3>32766 AND
        IS4>32766 AND WindSpeed<20 THEN M2.REV:= FALSE
        ; M2FWD:= FALSE; TltDeg:=TltDeg+Deg2; H:=2;
        Counter2:=0; Deg2:=0;
261     ELSIF I=12 AND H=2 AND Deg2<6 AND IS3>32766 AND
        IS4>32766 AND WindSpeed<20 THEN M2FWD:= FALSE
        ; M2.REV:= TRUE; P2:=Power;
262     ELSIF I=12 AND H=2 AND Deg2>6 AND WindSpeed<20
        THEN M2FWD:= FALSE; M2.REV:= FALSE; TltDeg:=
        TltDeg-Deg2; I:=13; H:=0; Counter2:=0; Deg2
        :=0;
263     END_IF;
264     P2Max:= MAX(P0,(MAX(P1,P2)));
265 END_IF
266 IF WindSpeed>20 THEN I:=100; //Moved from bottom of IF-
        statement due to Structured Text prioritization
267 ELSIF I=13 AND P2Max=P2 AND WindSpeed<20 THEN M2FWD:=
        FALSE; M2.REV:= FALSE; Delay(IN:=TRUE, PT:=T#60S); IF
        NOT(Delay.Q) THEN RETURN; END_IF Delay(IN:=FALSE); P0
        :=0; P1:=0; P2:=0; P3:=0; Counter2:=0; Deg2:=0; I:=10;
268 ELSIF I=13 AND P2Max = P0 AND WindSpeed<20 AND Deg2<3
        THEN M2.REV:= FALSE; M2FWD:= TRUE;
269 ELSIF I=13 AND P2Max = P0 AND WindSpeed<20 AND Deg2>3
        THEN M2.REV:= FALSE; M2FWD:= FALSE; Delay(IN:=TRUE,
        PT:=T#60S); IF NOT(Delay.Q) THEN RETURN; END_IF Delay(
        IN:=FALSE); P0:=0; P1:=0; P2:=0; P3:=0; TltDeg:=TltDeg
        +Deg2; Counter2:=0; Deg2:=0; I:=10;
270 ELSIF I=13 AND P2Max= P1 AND WindSpeed<20 AND Deg2<6 THEN
        M2.REV:= FALSE; M2FWD:= TRUE;
271 ELSIF I=13 AND P2Max= P1 AND WindSpeed<20 AND Deg2>6 THEN
        M2.REV:= FALSE; M2FWD:= FALSE; Delay(IN:=TRUE, PT:=
        T#60S); IF NOT(Delay.Q) THEN RETURN; END_IF Delay(IN:=
        FALSE); P0:=0; P1:=0; P2:=0; P3:=0; TltDeg:=TltDeg+
        Deg2; Counter2:=0; Deg2:=0; I:=10;
272 ELSIF I=13 AND Power<200 AND Windspeed<20 AND
        sun_elevation >=10 THEN I:=201;
273 ELSIF I=13 AND sun_elevation <10 AND Windspeed<20 THEN I
        :=300;
274 END_IF
275 //IF WindSpeed>1 THEN I:=100; X:=0; Delay(IN:=FALSE);

```

END_IF

B PLC code written in this thesis

```
1  //(Input/32760)*10 is Wago 750–468 data to voltage
   conversion (see manual).
2  Windspeed:= (AM/32760)*10*0.164; //Sensitivity of
   anemometer is 0.165 Vs/m
3  Irrad:= (PM/32760)*10*49.5; //Sensitivity of Pyranometer
   is 49.5 mV*m^2/W
4  //Raw input data for voltage and current
5  Raw_Voltage_Input:= IoConfig_Globals.Mapping.Voltage;
6  Raw_Current_Input:= IoConfig_Globals.Mapping.Current;
7  //Calculating input voltage and current
8  Voltage_Rm:= 329; //Measured value using multimeter
9  Voltage_Pre_Resistor_Rm:= 39875; //Measured value using
   multimeter
10 Voltage_LEM_Voltage := (Raw_Voltage_Input/32760)*10; //
   Value of 32760 corresponds to 10V input (found in
   module manual), multiply by 10 because it measures
   +-10V.
11 Voltage_measured:= (Voltage_LEM_Voltage/Voltage_Rm)*0.4*
   Voltage_Pre_Resistor_Rm; // 0.4 is 1000/2500 (LEM
   Element turns ratio reversed) because PLC seemingly
   cannot calculate it otherwise
12 Current_Rm:= 149.1; //Measured value using multimeter
13 Current_LEM_Voltage := (Raw_Current_Input/32760)*10; //
   Value of 32760 corresponds to 10V input (found in
   module manual), multiply by 10 because it measures
   +-10V.
14 Current_measured:= (Current_LEM_Voltage/Current_Rm)
   *(1000/1); //1000/1 is LEM Element turns ratio
   reversed
15 Power:= Voltage_measured*Current_measured;
16 //Calculation of solar position
17 time_zone := 1; //Timezone set to CET always at request
   of supervisor
18 //time_zone := Time_And_Date.TimeZone.iOffset/60; //
   Variable timezone (auto-switch between CET AND CEST)
19 Time_And_Date:= WagoAppTime.FuGetLocalTimeComponents();
   // Puts time and date data into the Time_And_Date
   struct
20 month := Time_And_Date.uiMonth;
21 day := Time_And_Date.uiDay;
22 hour := Time_And_Date.uiHour;
23 minute := Time_And_Date.uiMinute;
```

```

24 second := Time_And_Date.uiSecond;
25 day_of_year := Time_And_Date.uiYday;
26 IF WagoAppTime.FuIsLeapYear(Time_And_Date.uiYear) THEN //
    Checks for leap year, relevant to calculation
    algorithm
27     days_in_year:= 366;
28 ELSE
29     days_in_year:=365;
30 END_IF
31 y := (2*pi/days_in_year)*(day_of_year - 1 +((hour-12)/24)
    );
32 eqtime := 229.18*(0.000075 + (0.001868*COS(y)) -
    (0.032077*SIN(y)) - (0.014615*COS(2*y)) - (0.040849*
    SIN(2*y)));
33 decl_rad := 0.006918 - 0.399912*COS(y) + 0.070257*SIN(y)
    - 0.006758*COS(2*y) + 0.000907*SIN(2*y)
34 - 0.002697*COS(3*y) + 0.00148*SIN(3*y);
35 decl_deg := decl_rad * (360/(2*pi));
36 time_offset := eqtime + (4*longitude_deg) - (60*time_zone
    );
37 tst := (hour*60) + minute + (second/60) + time_offset;
38 ha_deg := (tst/4) - 180;
39 ha_rad := ha_deg * ((2*pi)/360);
40 zenith_rad := ACOS((SIN(latitude_rad)*SIN(decl_rad)) + (
    COS(latitude_rad)*COS(decl_rad)*COS(ha_rad)));
41 theta_rad := -ACOS(-((SIN(latitude_rad)*COS(zenith_rad)-
    SIN(decl_rad))/(COS(latitude_rad)*SIN(zenith_rad)))+
    pi);
42 theta_deg := theta_rad * (360/(2*pi));
43 sun_elevation := 90 - (zenith_rad*(360/(2*pi)));
44 sun_azimuth := theta_deg+180;
45 //SOLAR TRACKING MODE BASED ON TIME
46 //Enters solar tracking mode from state 13
47 IF I=201 AND Power<200 AND Windspeed<20 AND sun_elevation
    >=10 THEN
48     IF (sun_azimuth-1)<AziDeg AND AziDeg<(sun_azimuth
        +1) THEN M1FWD:=FALSE; M1REV:=FALSE; I:=202;
        // 1 degree around actual
49     ELSIF AziDeg < sun_azimuth THEN M1FWD:=TRUE;
        M1REV:=FALSE; // sun azimuthal angle where it
        doesn't move to prevent
50     ----- ELSIF AziDeg->-sun_azimuth THEN M1FWD:=FALSE; -
        M1REV:=TRUE; -// the rig from constantly moving back -
        and forth
51     ----- END_IF
52 ELSIF I=202 AND Power<200 AND Windspeed<20 AND

```



```

        sun_elevation >= 10 THEN
53  ----- IF ( sun_elevation - 1) < TltDeg AND TltDeg < (
        sun_elevation + 1) THEN M2_FWD := FALSE; M2_REV := FALSE;
54  ----- ELSIF TltDeg < sun_elevation THEN M2_FWD := TRUE;
        M2_REV := FALSE;
55  ----- ELSIF TltDeg > sun_elevation THEN M2_FWD := FALSE;
        M2_REV := TRUE;
56  ----- END_IF
57  ELSIF ( I = 201 OR I = 202) AND Power >= 200 THEN
58  ----- M1_FWD := FALSE; M1_REV := FALSE; M2_FWD := FALSE;
        M2_REV := FALSE; I := 10;
59  END_IF
60  //STAND-BY-MODE-WHEN-SUN-IS-DOWN
61  // Enters stand-by mode from state 13
62  IF I = 300 THEN M1_FWD := FALSE; M1_REV := FALSE; M2_FWD := FALSE
        ; M2_REV := FALSE;
63  ELSIF I = 300 AND sun_elevation >= 10 THEN I := 201;
64  END_IF
65  // As well as miscellaneous code modified and added to
        remove bugs

```

C PLC module wiring list

Table C.1: PLC module wiring list [4]

Pin Name/Number	Connected to
Motor 1, +24V	H-Bridge (Motor1 +)
Motor 1, 0 V	H-Bridge (Motor 1 -)
Hall Sensor 1, Pin 1: 0 V	PLC 750-404/1 (0 V)
Hall Sensor 1, Pin2: +24 V	PLC 750-404/1 (24 V)
Hall Sensor 1, Pin3: Signal	PLC 750-404/1 (CLK)
Motor 2, +24V	H-Bridge (Motor2 +)
Motor 2, 0 V	H-Bridge (Motor 2 -)
Hall Sensor 2, Pin 1: 0 V	PLC 750-404/2 (0 V)
Hall Sensor 2, Pin2: +24 V	PLC 750-404/2 (24 V)
Hall Sensor 2, Pin3: Signal	PLC 750-404/2 (CLK)
Induction Sensor 1, 24V	PLC (24 V)
Induction Sensor 1, Signal	PLC 750-455/1 (A1)
Induction Sensor 2, 24V	PLC (24 V)
Induction Sensor 2, Signal	PLC 750-455/1 (A2)
Induction Sensor 3, 24V	PLC (24 V)
Induction Sensor 3, Signal	PLC 750-455/1(A3)
Induction Sensor 4, 24V	PLC (24 V)
Induction Sensor 4, Signal	PLC 750-455/1 (A4)
Pyranometer, +	PLC 750-468 (A1)
Pyranometer, -	PLC 750-468 (GND)
Anemometer, +24V	PLC (24 V)
Anemometer, 0V	PLC (0 V)
Anemometer, Signal	PLC 750-468 (A2)
H-Bridge, 24V +	24 V Power source (+24 V)
H-Bridge, 24V -	24 V Power source (GND)
H-Bridge, FWD_SIG1 (1)	PLC 750-504 (D1)
H-Bridge, FWD_SIG1 (2)	PLC 750-504 (V0)
H-Bridge, REV_SIG1 (1)	PLC 750-504 (D2)
H-Bridge, REV_SIG1 (2)	PLC 750-504 (V0)
H-Bridge, FWD_SIG2 (1)	PLC 750-504 (D3)
H-Bridge, FWD_SIG2 (2)	PLC 750-504 (V0)
H-Bridge, REV_SIG2 (1)	PLC 750-504 (D4)
H-Bridge, REV_SIG2 (2)	PLC 750-504 (V0)
PV out	Current measuring device
PV out	Voltage measuring device
Voltage measuring device, Signal	PLC 750468/2 (A1)
Current measuring device, Signal	PLC 750468/2 (A2)

D Relay turn off current graphs

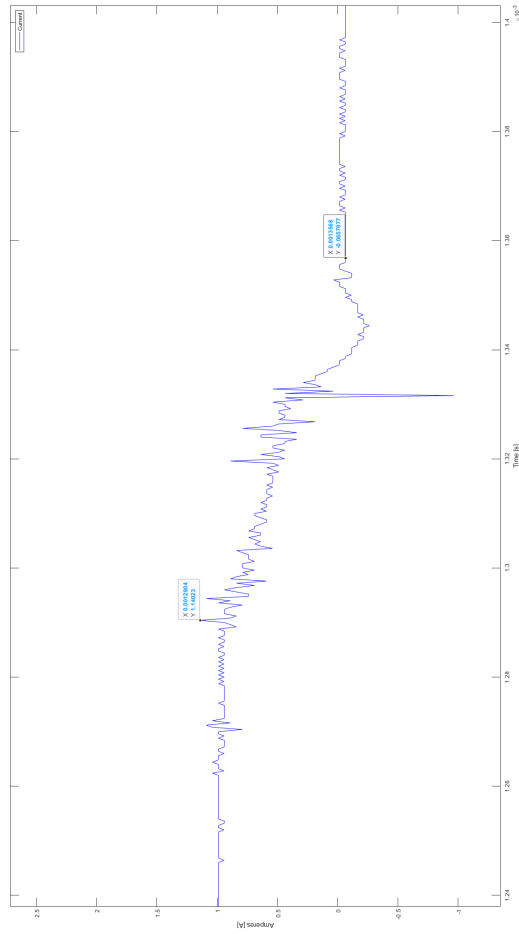


Figure D.1: Test 1: Relay current when switching H-bridge off used to approximate capacitance needed

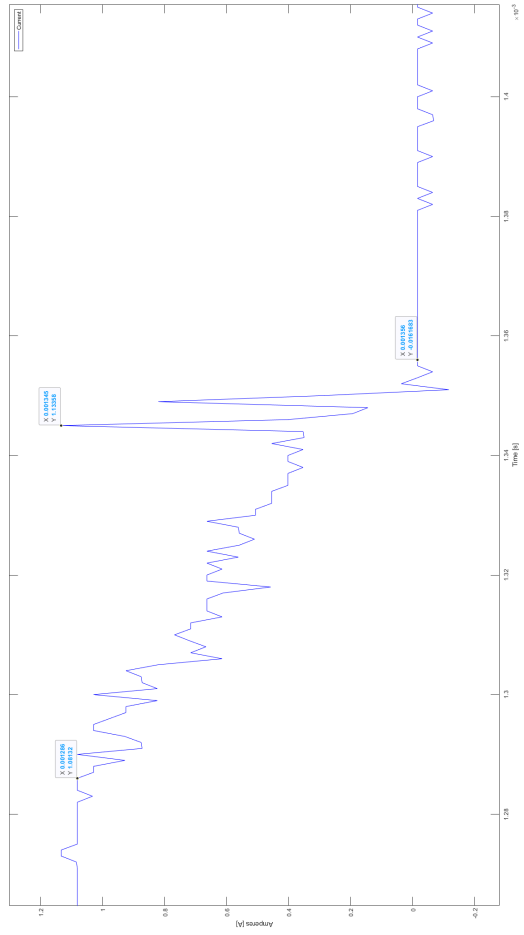


Figure D.2: Test 2: Relay current when switching H-bridge off used to approximate capacitance needed

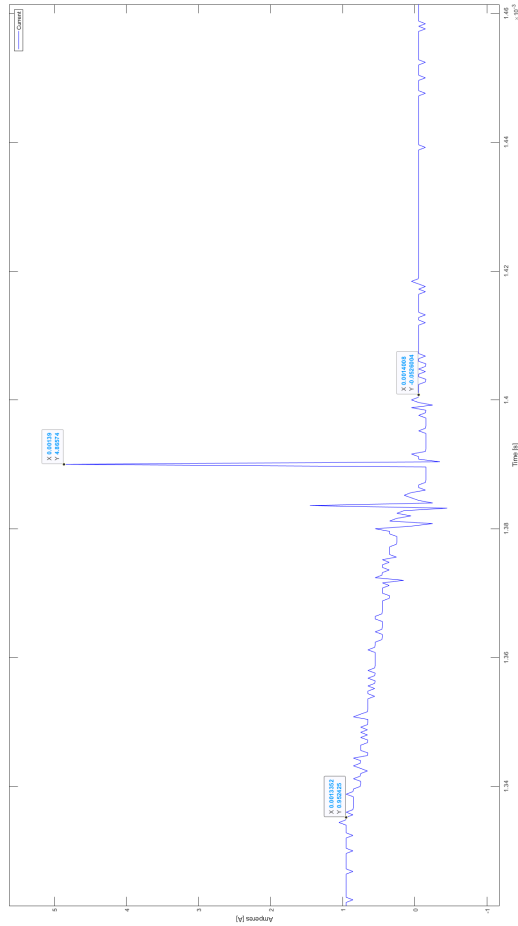


Figure D.3: Test 3: Relay current when switching H-bridge off used to approximate capacitance needed

E H-bridge simulation schematic

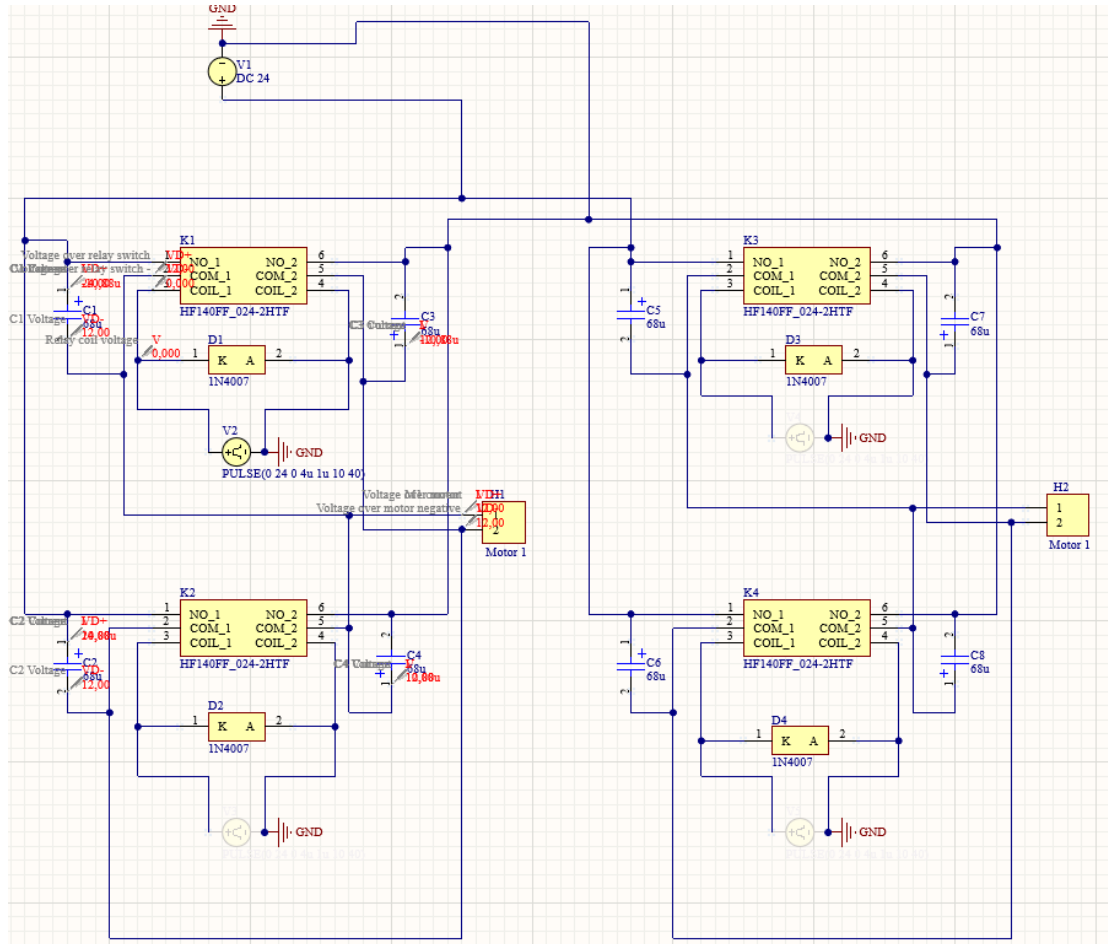


Figure E.1: H-bridge schematic used to simulate as shown in Altium Designer

F Motor start current and voltage

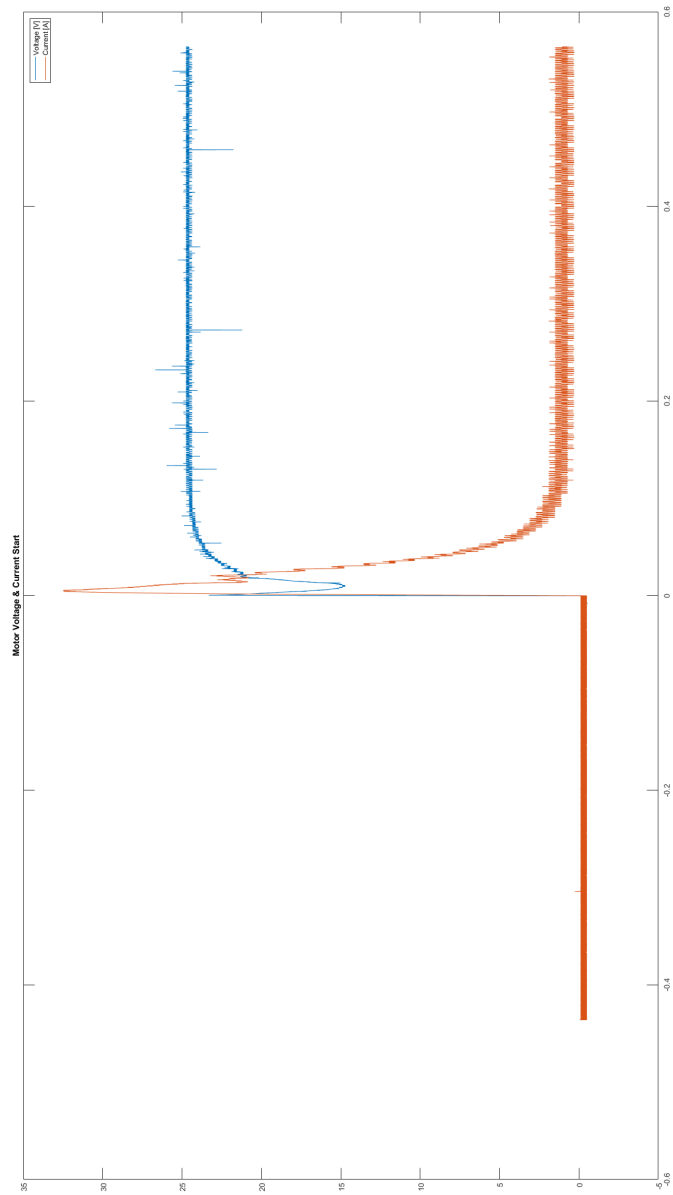


Figure F.1: Motor start-up voltage and current, where the blue line is voltage and red is current

